Murdoch University

THESIS

Utilising antigen-antibody complexes for the immunomagnetic enrichment of spermatozoa from sexual assault intimate swabs.

Sara NATALE
33432899

This thesis is presented for the degree of

Accelerated Master of Forensic Biotechnology (Research with Training)

in

Medical, Molecular and Forensic Sciences

Murdoch University

Sara Natale, Dr Andrew Currie, and Brendan Chapman

2021

Murdoch University

Statement of Candidate Contribution

I declare that this thesis is my own account of my research and contains its main content work which has not previously been submitted for a degree at any tertiary education institution.

Sara Natale

(Student)

murdoch.edu.au

CRICOS provider code:00125J

Abstract

Sexual assault is prevalent within today's society with 18% of women reporting sexual assault within their lifetime (1). Physical evidence collected from a forensic examination may include an intimate swab. The standard method used for sperm isolation is differential lysis however, the high abundance of vaginal epithelial cells on vaginal sexual assault swabs complicates the protocol. This factor results in mixed DNA profiles with an overabundance of female DNA present in an autosomal STR profile. Mixed STR profiles make it difficult to interpret the male DNA profile and therefore cannot always be used in court to identify a perpetrator. An antibody-based method for spermatozoa extraction using antibody conjugated immunomagnetic beads to select for sperm could be used as a method of enrichment, producing a higher yield of recovered male DNA. To achieve this, sperm-specific antibodies are needed to selectively bind to the sperm when in an epithelial/sperm cell mixture.

This study aimed to identify the capability of 3 antibodies, α-SPAM1, α-SPACA1, and α-ZPBP with a secondary antibody Goat α-Rabbit IgG (H+L) Secondary Antibody, Alexa Fluor Plus 488 through flow cytometry. Canto™ II CA flow cytometer was used for the visualisation of sperm/vaginal epithelial cell cross-reactivity with the antibodies to determine the cell sensitivity and selectivity. Optimisation of the flow cytometry protocol was undertaken for both the epithelial and sperm cells. The antibodies had >20% cross-reactivity to the sperm cells and >30% to the vaginal epithelial cells however, the epithelial cells had a higher autofluorescence than expected with >30% positive unstained epithelial cells.

Table of Contents

1. Review of the Literature 1
1.0 Introduction 1
1.1 Prevalence of sexual assault cases and ejaculation 1
1.2 Clinical Management 4
1.2.1 Clinical Management of Sexual Assault in Australia 5
1.2.2 Clinical Management of Sexual Assault in United Kingdom 5
1.2.3 Clinical Management of Sexual Assault in United States 7
1.3 Sperm Anatomy 8
1.4 Vaginal Epithelia 9
1.4.1 VK2/E6E7 (ATCC CRL-2616) – Vaginal Epithelial Cells 9
1.5 Sperm extraction techniques from sexual assault samples 10
1.5.1 Differential Extraction 11
1.5.2 Modifications to Differential Lysis 12
1.5.3 Challenges of Differential Extraction and Alternative Approaches 12
1.5.4 Nuclease-Based Approach 13
1.5.5 Alternative Approaches 13
1.5.6 Kit-Based Methods 13
1.5.7 Laser-Based Methods 15
1.5.8 Microdevices 15
1.5.9 Antibody-Based Methods 16
1.6 Antibodies 17
1.6.1 α-Sperm Adhesion Molecule 1 (SPAM1) 17
1.6.2 α-Sperm Acrosome Associated 1 (SPACA1) 18
1.6.3 α-zona pellucida binding protein 1 (ZPBP1) 18
1.7 Flow Cytometry 21
1.7.1 Aims and Hypotheses of the thesis 22
2. Methods 24
2.1 Study Participants 24
2.2 Specimen Storage 24
2.3 Sperm Counting 24
2.4 VK2/E6E7 (ATCC CRL-2616) Epithelial Cell Culture 25
2.5 FLOQSwab® saturation experiment 26
2.6 Determination of epithelial cell binding to FLOQSwabs® 26
2.7 Flow cytometry analysis 26

2.7.1 Primary Antibodies 26
2.7.2 FACS buffer 28
2.7.3 Optimisation of epithelial cell viability 28
2.7.4 Flow cytometry assay 28
2.7.5 Flow cytometry Analysis 28
3. Results 29
3.1 FLOQSwab® saturation experiment 29
3.2 Determination of epithelial cell binding to FLOQSwabs® 29
3.3 Flow cytometry 31
3.3.1 Flow cytometry gating strategy 31
3.3.2 Optimisation of epithelial cell viability and live/dead dye 32
3.3.4 Flow voltage optimization 39
3.3.5 Epithelial and sperm cell cross-reactivity with α-SPAM1, α-SPACA1, and α-ZPBP1 cocktail 41
4. Discussion 46
4.1 Epithelial cell binding and saturation of FLOQSwab® 46
4.2 Optimisation of epithelial cell viability and live/dead dye 46
4.3 Epithelial cell cross-reactivity with Secondary Antibody Alexa Fluor 488 47
4.4 Optimisation of flow voltage and epithelial/sperm cell cross-reactivity with α-SPAM1, α-SPACA1, and α-ZPBP1 cocktail. 47
4.5 Limitations 48
4.6 Conclusion 49
5. References 50

Murdoch University

List of Figures

Figure 1: The timeline of a victim alerting the police of a sexual assault. The timeline starting from contacting the police through to processing the early evidence kits within the crime laboratory, then to identify a perpetrator. The early evidence kit includes urine sample pots, mouth/vaginal swabs and mouth rinses (22). 6

Figure 2: Labelled diagram of human spermatozoa. Detailing the acrosomal region with an "A" in which the SPACA, ZPBP, and SPAM antigens are located. The front and side view are presented to demonstrate the sperms morphology (17). 9

Figure 3: A mixed Profile in Autosomal STR (male and female). by using identifier plus kit having 16 markers showing the low peaks of male, due to low quantity of male DNA and high peaks due to high quantity of female DNA (victim) Example Marker D2S1338 showing the male fraction peaks 17 and 22 while 18 and 23 of female fraction (33). 11

Figure 44: Visual diagram of the conventional differential lysis protocol. It begins with cutting a portion of the intimate swab and the addition of the of the epithelial cell lysis reagents, degrading the non-sperm fraction. Following incubation and centrifugation the supernatant is removed and sperm cell lysis reagents added. During incubation, the sperm cells will break open and release the male DNA (3). 11

Figure 55: Screening of different primary antibodies for sperm binding under optimised flow cytometry conditions. Sperm was stained respectively with 0.01 mg/mL of each primary antibody: α-SPACA1, α-SPAM1, α-ACR, α-TEKT1 and α-ZPBP. A) Global mean fluorescence intensity (MFI). B) Percentage of positive cells. Data shown are mean and standard deviations from n=1 donor from a single experiment, performed in duplicate. 2°= secondary antibody (1:1200) (81). 19

Figure 6: Diagram displaying the internal working of a flow cytometer. The sample in entered through the single cell suspension tube and transported through the machine using the fluidics system. The argon-ion laser, collection optics and forward light scatter detector are included in the optics system, before the data output onto a computer by the electronic system (83). 21

Figure 7: Haemocytometer grid to count sperm cells. The top corner of the grid outlined in red are the 16 squares used to calculate the concentration of sperm (89). 25

Figure 8: Epithelial cell recovery (cells/swab) from FLOQSwabs®. Using the protocol as per section 2.6 to determine the vaginal cell recovery of saturated FLOQSwabs®. Number of cells per swab was calculated by converting the cells/mL to cells/μL and multiplying the cell recovery by the eluted volume. Conditions throughout the experiment remained consistent as swabs were saturated, centrifuged and counted using trypan blue staining. 30

Figure 9: Flow cytometry gating strategy. Live vaginal epithelial cells were unstained with the absence of the fixable viability dye, Alexa Fluro 488, and all primary antibodies. A) forward-scatter by side-scatter graph of unstained vaginal epithelial cells. B) side-scatter width by side-scatter height graph of unstained epithelial cells C) fixable viability dye (APC-Cy7) histogram with gate set at 1.56. 32

Figure 10: Percentage of positive cells for fixable viability stain (APC-Cy7). A gate of 1.61 was set for the unstained sample and applied to the other samples within the experiment to measure positively stained cells. 34

Figure 11: Comparison of live and dead epithelial cells. The control are the live unstained cells to compare the difference when the stain is added to the cells. The data is the percentage of dead cell with in the third quadrant gate (presented as section "C" in Figure 11). 34

Figure 12: Back-gating strategy and comparative graphs. A) forward-scatter by side-scatter graph. B) side-scatter width by side-scatter height graph. C) fixable viability dye by side-scatter with four quadrant gates. D) viability dye effectiveness comparing live and dead stained samples. Histogram of fixable viability dye. E) Dead samples stained with fixable viability dye from three initial experiments, comparing populations. 35

Figure 13: The cross-reactivity of Alexa Fluro 488 (2° antibody) on epithelial cells. The live unstained data was gated at 1.60 and the dead unstained cells at 1.50 as the controls. A) Percentage of positive cells within the samples. B) Global mean fluorescence intensity (MFI). The analysis from the unstained samples were copied into the remaining data. The experiment was conducted as per section 2.7.4. 37

Figure 14: Cross-reactivity of Alexa Fluro 488 on epithelial cells with back-gating strategy. The live unstained data was gated at 1.60 and the dead unstained cells at 1.50 as the controls. A) forward-scatter and side-scatter area. B) side-scatter width by side-scatter height, to determine granularity. C) Alexa Fluro 488 by fixable viability dye, to determine the staining fluorescence. D) Alexa Fluro 488 positive cell binding gate for live epithelial cells stained with fixable viability dye and 2° antibody. E) Alexa Fluro 488 positive cell binding gate for dead epithelial cells stained with fixable viability dye and 2° antibody. 38

Figure 15: Optimization of flow cytometry voltages displaying epithelial and sperm cells. A) Live epithelial cells set at the linear epithelial voltage. B) Live sperm cells set at linear epithelial voltage. C) Live epithelial cells set at linear sperm voltage. D) Live sperm cells set at linear sperm cell voltage. E) Live mixed cell sample (epithelial and sperm cells) set at log voltage. No samples contained any primary or secondary antibodies. 40

Figure 16: Cross-reactivity of sperm and epithelial cells to the α-SPAM1, α-SPACA1, and α-ZPBP1 antibody cocktail using Alexa Fluro 488 for visualization. A) 2° antibody by forward-scatter of the mixed sample stained with the antibody cocktail, viability dye and Alexa Fluro 488. B) 2° antibody by forward-scatter of the sperm cell sample stained with the antibody

cocktail, viability dye and Alexa Fluro 488. C) 2° antibody by forward-scatter of the epithelial sample stained with the antibody cocktail, viability dye and Alexa Fluro 488. D) Alexa Fluro 488 histogram of positive cells in the mixed sample stained with the antibody cocktail, viability dye and Alexa Fluro 488. Data collected from quadrant four. E) Alexa Fluro 488 histogram of positive cells in the mixed sample stained with the antibody cocktail, viability dye and Alexa Fluro 488. Data collected from quadrant three. 42

Figure 17: The binding-efficiency of sperm and epithelial cells to α-SPAM1, α-SPACA1, and α-ZPBP1 antibody cocktail using Alexa Fluro 488 for visualization. Flow cytometry protocol as per section 2.7.4 remained consistent throughout the experiment. A) Cell frequency percentage of sperm cells (quadrant one). B) Global MFI of sperm cells. C) Cell frequency percentage of epithelial cells (quadrant two). D) Global MFI of epithelial cells. E) Percentage of positive cells from quadrant three analysis. Unstained sample was set at 1.54. F) Percentage of positive cells from quadrant four. The flow cytometer ran 30,000 events from each sample consistently. 45

List of Tables

Table 1: Prevalence (percentage) of sexual assault. Including penile penetration of the vagina among multiple demographics including, adults (18 - 50 years), children (up to 18 years of age), and the elderly (over 50 years old). Comparing Australia (2018), United States (2015), and global statistics. These statistics include reported cases overall and not specified into known and unknown perpetrators. Data does not include all sexual assault cases, only groups from specific studies (1)(5)(6)(7). 2

Table 2: Comparing prevalence of sexual assault involving penile penetration of the vagina among females (adults and children) among the population of differing continents. Comparing continent and age statistics with female victims. Female adults include those who are 18 and older and female children include those who are under 18. An elderly female is considered over the age of 65. Data does not include all sexual assault cases, only groups from specific studies (1)(7)(8). 2

Table 3: A comparison of sperm detection times and case percentages among penile penetration of the vagina, anus, and mouth. Comparing maximum detection times of intact sperm and sperm heads, percentage of condom use, ejaculation reported, cases with intact sperm, cases with sperm heads and cases with no sperm (12).......... 4

Table 4: Sperm Specific Primary Antibodies 20

Table 5: Primary and secondary antibody descriptions used in the study........... 27

Table 6: The total saturation volumes (µL) of FLOQSwabs®. The swabs were dipped in a tray with 10mL of water for 5 seconds. Then placed in spin baskets within a 1.5mL Eppendorf tube and centrifuged at 4226 rpm for 1, 1 minute 30 seconds, and 2 minutes. Five swabs tested for 1 minute, and 2 swabs tested for each 1 minute 30 seconds and 2-minute centrifugation. 29

Table 7: Mean and standard deviation of vaginal cell recovery from FLOQSwabs®. Using the protocol as per section 2.6 to determine the vaginal cell recovery of saturated FLOQSwabs®. Number of cells per swab was calculated by converting the cells/mL to cells/µL and multiplying the cell recovery by the eluted volume. 30

1. Review of the Literature

1.0 Introduction

Sexual assault is known as violence of a sexual manner involving acts of coerced or unwanted forced physical contact (1). Sexual assault can include acts ranging from unwanted sexual touching through to more invasive actions such as various types of penetration (e.g. vaginal, anal, oral, digital and oral), with penile penetration being the most common form of penetrative assault (2). In Australia, 97% of sexual assault perpetrators in 2016 reported to the police were male (1). Females who present to a sexual assault health centre following an act of sexual violation, including penile penetration of the vagina, undergo a female intimate swab as part of a greater forensic examination. An intimate swab is an internal swab of the vagina used to obtain a forensic sample providing evidence of penetration regarding the presence of semen and therefore, resulting in a DNA profile. Once the swab is taken, it is then stored and taken to a crime laboratory where the specimen will be tested for the presence of deoxyribonucleic acid (DNA) from perpetrator sperm cells. Due to the abundance of female DNA present in the sample, it is important to separate the sperm cells from female vaginal (and other) cells before DNA analysis occurs. Generally, this is accomplished through differential extraction of male DNA (the gold standard method of DNA extraction) however, recent evidence suggests limitations of the method, which can produce unusable results for court (3). Therefore, it is imperative that new extraction methods are explored which produce higher yields of perpetrator DNA. A method of extraction which will be explored in this thesis includes the use of specific antibodies to attract the sperm away from the vaginal cells in the sample and capture them with immunomagnetic beads.

1.1 Prevalence of sexual assault cases and ejaculation

Sexual assault can occur to individuals other than women such as, men, gender diverse individuals, children, elderly, and those assigned male at birth but is a woman (and vice versa) (4). Women have the highest prevalence of sexual assault, with 18% of Australian women compared to 4.7% of men reporting sexual assault in their lifetime (1). The prevalence of sexual assault involving penile penetration of the vagina is demonstrated in Table 1 and compared among multiple demographics. The prevalence of vaginal assault in children can also be compared among continents and age groups as seen in Table 2, to highlight the severity of penetrative sexual assault among the range of demographics.

Table 1: Prevalence (percentage) of sexual assault. Including penile penetration of the vagina among multiple demographics including, adults (18 - 50 years), children (up to 18 years of age), and the elderly (over 50 years old). Comparing Australia (2018), United States (2015), and global statistics. These statistics include reported cases overall and not specified into known and unknown perpetrators. Data does not include all sexual assault cases, only groups from specific studies (1)(5)(6)(7).

	Australian adults (18 - 50 years)	Australian children (<18 years)	United States adults (18 - 50 years)	United States elderly females (50+ years)	Children globally (<18 years)
Cases reported with female victims (%)	18	22	21	6	12

Table 2: Comparing prevalence of sexual assault involving penile penetration of the vagina among females (adults and children) among the population of differing continents. Comparing continent and age statistics with female victims. Female adults include those who are 18 and older and female children include those who are under 18. An elderly female is considered over the age of 65. Data does not include all sexual assault cases, only groups from specific studies (1)(7)(8).

	Australia	Africa	Europe	Canada /USA	New Zealand
Reported sexual assault cases within the continent with female victims over 18 years (% of entire population)	18	-	11.7	8.1	14.1
Reported sexual assault cases within the continent with female victims <18 years (% of entire population)	21.5	20.2	13.5	20.1	-

It is important to note that statistics regarding prevalence of sexual assault is reliant on victim reporting rates, and there may be many cases which have gone unreported (7). The SARS-CoV-2 global pandemic has affected sexual assault rates, as there has been a general

reduction of cases with known assailants (9). Sexual and physical assault cases presenting to emergency departments decreased by approximately 50% due to quarantine in 2020, compared to the same month in 2018 (9). Sexual assaults can occur almost everywhere, including the victim's home, the assailant's home, automobiles, outdoors or public buildings. Individuals who experienced sexual assault in their own homes would most likely have had a known assailant or intimate partner assault them (9). Outdoor assaults are more commonly committed by unknown offenders (from 5.19% in 2018 to 22.86% in 2020) (9). Sexual assault against women commonly occurs indoors (89% of cases) with only 11% of cases occurring outdoors (10).

In some cases, weapons can be used in conjunction with a sexual assault. These weapons often include a knife or a gun, which are more commonly used by a stranger assailant (11). There are numerous forms of sexual assault which both men and women experience. In a study of 1,076 sexual assault cases, vaginal assault presented as the most common with 83% of women experiencing this type of assault. Oral assault appeared more common with men as 43% of male victims compared to 25% of female victims. Anal assault was more prevalent with male victims (67%), than female victims (15%) (11).

Male ejaculation occurs in approximately 53% of sexual assault cases involving penile penetration of the vagina (12). The average male ejaculate has a volume of 2-5mL containing 10^7 to 10^8 spermatozoa per millilitre (12). The female human body degrades semen through phagocytic process with mononuclear cells and neutrophilic lymphocytes within the vagina (12). The sperm tail is usually the first piece of the sperm to degrade, whereas the sperm head degrades last which can be seen on Table 3 (12). The percentage of vaginal penetration cases with intact sperm present versus cases with sperm heads present is 20% and 75% respectively (Table 3). The maximum time post-assault for the detection for sperm heads, amongst vaginal penetration assaults is 84 hours, and anal assault 40 hours. Oral assault can capture sperm heads up to 21 hours after occurrence with an oral swab (12).

Table 3: A comparison of sperm detection times and case percentages among penile penetration of the vagina, anus, and mouth. Comparing maximum detection times of intact sperm and sperm heads, percentage of condom use, ejaculation reported, cases with intact sperm, cases with sperm heads and cases with no sperm (12).

Penetrated area	Max. Detection Time (Hours)	Condom Use (%)	Ejaculation Reported (%)	Cases with Intact Sperm (%)	Cases with Sperm Heads (%)	Cases with no Sperm (%)
Vagina	Intact Sperm – 31 Sperm Heads – 84	6	53	20	75	5
Anus	Intact Sperm – 1.5 Sperm Heads – 40	4	27	0	65	17
Mouth	Sperm Heads – 21	0	22	0	34	83

1.2 Clinical Management

Females who present to a sexual assault health centre following a sexual violation including penile penetration of the vagina, will undergo a forensic examination (e.g., female intimate swab). There are at least two types of samples that can be collected from female genitalia used to detect semen from the vagina. These are an external labial and a high vaginal sample. Both samples have slightly different methods of collection however, both include the use of a swab (13). The external labial sample is taken directly with a swab, though the high vaginal sample includes interventions to open the external vagina to access the high vaginal area for a deeper swab sample. A wet swab requires a few drops of sterile water to moisten it before taking the sample, a dry swab may then follow. An intimate swab is an internal swab of the vagina to obtain a forensic sample regarding evidence of penetration (e.g., presence of semen) (13). The optimal timeframe for forensic sample collection of penile penetration from a female, ranges from within 24 hours to 72 hours as the yield of sperm will begin to decrease (14). Semen may still be present for up to five days (15). The longer the victim takes to present for forensic examination the less sperm will be present on the swab, resulting in amounts too low for accurate detection of DNA analysis. (15). A forensic examination must be completed by a trained nurse or doctor when conducted within the hospital emergency department (15).

1.2.1 Clinical Management of Sexual Assault in Australia

In Australia once an individual has experienced a sexual assault, they will seek the appropriate resources, including the Sexual Assault Resource Centre (SARC). Individuals should first present themselves to primary care, for example the emergency department within a hospital, or a sexual assault health centre (e.g., Western Australia has SARC). SARC provides counselling, medical, and forensic support to individuals who have experienced a sexual assault within 14 days of occurrence (16). SARC's priority of patient care is to address any major health issues. If any major health issues are revealed the patient will be sent directly to an emergency department for the proper medical care they require. If no major health issues are a risk to the patient, the SARC doctors, with the consent of the patient, provide reassurance, treatment, advice, and follow-up regarding injuries, sexually transmitted infections, or emergency contraception in case of pregnancy. The SARC doctors may examine those recently assaulted including, documentation (including photography), interpretations of injuries sustained, and the collection of intimate swabs. These examinations/documentations can be used if the case follows through legal proceedings. The forensic service is provided to the victim regardless of whether the sexual assault has been reported to the police. Physical evidence such as intimate swabs or photographs, can be stored for a period of up to three months (due to storage limits) in Australia, whereas medical records are kept indefinitely. SARC has supplied general practitioners and hospitals with forensic evidence collection kits and manuals within regional areas, to ensure sufficient care is given to all individuals (16). The duration of time it usually takes to complete all examinations and documentations at SARC is around 2-4 hours (16).

Different swabs are available for forensic use including cotton, nylon flocked, and Copan rayon swabs. Cotton swabs have an inadequate design for capturing and releasing epithelial and sperm cells, reducing the chance of a single-sourced STR profile. The fibres of a cotton swab are wrapped around the plastic shaft of the bud called a "mattress design" (17)(18). According to a 2018 study cotton swabs had 21.5% extraction efficiency of cellular material whereas, the nylon flocked swab had 48.4% extraction efficiency (19). Cotton swabs may be easily accessible however, residue cotton fibres left within the sample may have a negative effect on the STR profile (20). FLOQSwabs® used within this study have an alternative structure to cotton swabs as the tip is covered with perpendicularly sprayed on Nylon® fibres using the Copan's proprietary flocking process. The swab has no inner core for cells to become trapped in and therefore allows for effective cell uptake and elusion (21)(20).

1.2.2 Clinical Management of Sexual Assault in United Kingdom

The UK guidelines on the management of adult and adolescent victims of sexual assault, indicate that the needs of a patient presenting following a sexual assault can be classified as

immediate, medium, and longer term, depending on time of presentation. Immediate needs (disclosed within 7 days of the assault) are immediate safety, treatment of injuries, sexually transmitted disease (STI) prophylaxis, pregnancy prevention and forensic medical examination (FME) of the patient. If the assault is disclosed after 7 days, it is classified as medium-term needs. Medium term needs are STI screening, hepatitis B vaccination, pregnancy testing and identification of post-traumatic stress disorder. Further concerns regarding STI's and post-traumatic stress disorder are long term needs (disclosed after 1 year post-assault) (22).

The victims of the assault may be given a referral from the doctor in the emergency department for a specialized sexual assault service, for the appropriate forensic and psychosocial care (15). If the patient prefers, hospitals have forensic and mental health facilities on site. Not all victims of sexual assault may want to report the assault to the police and have forensic evidence gathered. A forensic medical examination involving the police may proceed as per Figure 1 (22).

Contact the local police

Specialist police officers (sexual assault management) will take a brief first account of the incident

Police arrange a foresnic medical examination

Officers may use an early evidence kit

Kit sent to a crime laboratory for testing

Figure 1: The timeline of a victim alerting the police of a sexual assault. The timeline starting from contacting the police through to processing the early evidence kits within the crime laboratory, then to identify a perpetrator. The early evidence kit includes urine sample pots, mouth/vaginal swabs and mouth rinses (22).

If a victim decides not to alert the police of the offence, they are still able to attend a sexual assault health centre and receive a FME and evidence collection. The options for non-police referrals include testing and storage of anonymous forensic samples, release of police intelligence information with and without samples, independent police officer advice, and the ability to revisit previous testing and reporting decisions (22).

1.2.3 Clinical Management of Sexual Assault in United States

The United States of America (U.S.) adapt a similar strategy to managing sexual assault cases as Australia. If the victim of a sexual assault tells an individual other than the police first, then they are known as the "outcry witness". Officers when alerted that a sexual assault has taken place should explain to the victim that evidence from the assault can be destroyed through showering, douching, bathing, brushing teeth or using mouthwash. The scene of a sexual assault (if applicable) should be protected and processed like any crime scene when there may be important evidence present. A follow-up investigation will be conducted by detectives within larger departments, where a victim statement interview is recorded on audiotape. The investigators involved should reassure the victim for their safety, as a priority, and remain in contact with the victim throughout the investigation. Cases involving children in the US use a different approach, as they cannot legally give consent under law. Children commonly disclose the assault to an outcry witness, which can follow with an investigation once the authorities are alerted (23). Just as Australia, the US also examines victims within an emergency room of a hospital; however, they have Sexual Assault Nurse Examiners and Sexual Assault Response Teams (19). The victims should be assessed medically and be examined for physical collection of evidence (e.g., photographs and intimate swabs), after consent is given. Consent must also be given by the victim to release the physical evidence collected, to the police. It is also important to obtain the appropriate documentation and obtain sufficient history from the victim for future reference. While being tested for the presence of semen the victims are often also tested for pregnancy and STI's as a precautionary measure (23). Generally physical evidence is collected from a "rape kit" or "sexual assault evidence collection kit", however clinicians are not bound by this as documentation and photography of injuries can also be included. Unless the assault occurred within 72 hours of the examination then complete evidence-collection protocols are not indicated (23). The U.S. generally conducts similar protocols to Australia when assessing/examining a sexual assault case, the main distinction is the differing laws of the countries.

Clinical management and collecting samples are the first steps following the occurrence of a sexual assault. To identify the perpetrator, the sample (intimate swab) must then go to a crime laboratory for testing. The laboratory will then undergo sperm extraction techniques to extract the DNA for identification.

1.3 Sperm Anatomy

Spermatozoa is a single cell that is comprised of a head, midpiece and tail region, bound by a plasma membrane, as seen in Figure 2. A typical sperm head is a pear shape, approximately 5 micrometres long, and 3 micrometres wide (24). The sperm head is divided into the anterior and posterior regions containing the acrosomal and post-acrosomal regions, respectfully. The nucleus is contained within the core of the sperm head and is composed of compressed chromatin with protamine's bound to the DNA (for protection again DNA damage) (24). The acrosome is a cap-like structure covering 40-70% of the sperm head and lies underneath the plasma membrane, and is important for female egg binding during fertilization (24)(25). Sperm cells haploid nature implies that they contain one set of chromosomes which is imperative for reproduction. An oocyte and sperm cell (each containing a single set of chromosomes) come together to form a diploid cell called a zygote containing two sets of chromosomes (26)(27).

A sperm protein, sperm adhesion molecule 1 (SPAM1) is found on the inner acrosomal membrane and the plasma membrane, as seen in Figure 2 (28). SPAM1 plays a role in three important functions during fertilization: cumulus (cells that surround and nurture oocytes) dispersion, secondary zona pellucida (ZP) binding after acrosome reaction and calcium signalling-associated acrosomal exocytosis (transportation and fusion of secretory vesicles) (28)(29)(30). Sperm acrosome membrane-associated protein 1 (SPACA1) can be found in a segment of the acrosome and functions as the expansion and establishment of the acrosome to assist in normal sperm morphology (30) . Zona pellucida binding protein 1 (ZPBP1) is located within the acrosome and works to bind to the oocyte zona pellucida. If ZPBP1 is not present in the male, then the sperm will appear to have an abnormal round-head and no forward motility (capable of movement) (31).

Figure 2: Labelled diagram of human spermatozoa. Detailing the acrosomal region with an “A” in which the SPACA, ZPBP, and SPAM antigens are located. The front and side view are presented to demonstrate the sperms morphology (17).

1.4 Vaginal Epithelia

While there are some studies, albeit outside of forensics, that have shown binding of α-SPACA1, α-SPAM1 and α-ZBPB1, there is little evidence of the ability of these antibodies bind in a mixed cell substrate. Epithelial cells, specifically vaginal epithelia, must demonstrate little to no binding for a α-SPACA1, α-SPAM1 and α-ZBPB1 cocktail to work.

Vaginal epithelial cells contain similar characteristics to those found elsewhere in the body (e.g., the mouth). One cell line is commercially available, VK2/E6E7 (ATCC CRL-2616).

1.4.1 VK2/E6E7 (ATCC CRL-2616) – Vaginal Epithelial Cells

A number of studies have used cheek buccal epithelial cells as an analogue for vaginal cells. The ectocervical and vaginal cell line (VK2/E6E7 (ATCC CRL-2616)) display stratified squamous non-keratinizing epithelia characteristics. Vaginal epithelial cells can be classified

into three different types: superficial intermediate, and parabasal cells. Superficial cells are the largest visible cells when viewing a microscopic vaginal smear, with a flat-looking display. Intermediate cells have a nearly rounded polygonal shape with visible nuclei, similarly to parabasal cells (32). Without any stimulation the cell line will produce prostaglandin E2, transforming growth factor beta1, polymeric immunoglobulin receptor, interleukin 8 and colony-stimulating factor (M-CSF) (33). The cells also come with a known autosomal DNA genotype (33).

1.5 Sperm extraction techniques from sexual assault samples

Before the male perpetrators DNA can be analysed, the spermatozoa must be separated or extracted from the female cells in the sample. Short tandem repeats (STRs) are repeated DNA sequences accounting for approximately 3% of the human genome (34). The number of repeat units between individuals vary making STR profiling a useful identification tool (35). If the sample is inadequately separated it can lead to detection of no male alleles and a greater abundance of female DNA in an resulting electropherogram (36). It may also lead to the generation of a mixed male/female DNA profile resulting in difficult interpretation as visualized in Figure 3 (36)(37). There are currently numerous different isolation and extraction methods used to analyse sexual assault intimate swabs. The gold standard method used throughout crime laboratories is differential extraction (38,39).

Figure 3: A mixed Profile in Autosomal STR (male and female). by using identifier plus kit having 16 markers showing the low peaks of male, due to low quantity of male DNA and high peaks due to high quantity of female DNA (victim) Example Marker D8S1179 showing the male fraction peaks 12 and 15 while 13 and 14 of female fraction (35).

1.5.1 Differential Extraction

The conventional method of differential extraction involves differential lysis of the of the sexual assault intimate swab sample (swab), to break open the female cells and release their DNA (genetic material) for subsequent removal. The lysis protocol should leave the sperm intact, as it uses proteinase K (Pro-K) and sodium dodecyl (SDS) for the initial digestion specifically targeting the epithelial cells and leaving the more robust sperm cells un-lysed (3). Prior to recovering the sperm cell pellet, the lysate (product of cell lysis) is then washed and centrifuged with the initial lysis solution (3). Using a surfactant (Pro-K and dithiothreitol; DTT) the sperm cell pellet is lysed to ideally release the perpetrators DNA (3). The differential lysis process is displayed in Figure 4. A study conducted by Gill et al.(40) on 100 semen-contaminated vaginal swabs resulted in a an insufficient mean success rate of 62% when using the differential lysis protocol (40).

Figure 44: Visual diagram of the conventional differential lysis protocol. It begins with cutting a portion of the intimate swab and the addition of the of the epithelial cell lysis reagents, degrading the non-sperm fraction. Following incubation and centrifugation the supernatant is removed and sperm cell lysis reagents added. During incubation, the sperm cells will break open and release the male DNA (3).

1.5.2 Modifications to Differential Lysis

The original differential lysis protocol (involving one wash step) resulted in female cells contaminating the final male fraction creating a mixed STR profile (40). The step was then modified with numerous washes, to improve epithelial cell elimination (40). Following further research, the increased wash steps were leading to increasing loss of sperm and damage to sperm cells, decreasing the male DNA yield (36)(41). The results suggested that further modifications were necessary for the optimization of the differential extraction protocol to enhance purity while retaining yield (36). The modifications included altering the incubation conditions, initial lysis buffer, and substituting washing steps with selective digestion (36). Most modifications resulted in no significant improvements however, altering the incubation temperature to <56°C was strongly suggested to increase sperm recovery (36). Other methods have also been studied including kit-based methods (38)(42)(43)(44), automation (45)(46), laser-based methods (47)(48)(49), microdevices (50)(51)(52)(53), and affinity-based methods (54)(55)(56).

Altering the detergents to anionic solutions such as 1% SDS produced the best results with 75% sperm recovery when compared to the differential extraction buffer with 40% recovery (57). The alteration of the incubation time, produced no significant results, whereas lowering the incubation temperature below 56°C increased sperm recovery (36).

1.5.3 Challenges of Differential Extraction and Alternative Approaches

The main limitation of the modified differential extraction method remains to be the carryover of the female DNA fraction in a mixed sample. The methods require extensive handling and are time-consuming for laboratories. The intricate steps of washing and digesting the sample add difficulty to the protocol. Over-washing the sample can result in a loss of male DNA and increases the chance for contamination. Whereas, under-washing a sample can result in increased amounts of epithelial cells that carryover into the male fraction of the STR profile. Similarly, if the lysis is inadequate the epithelial cells will remain intact, contaminating the male fraction of the mixed sample. Whereas, if the digestion is too harsh the sperm cells may be prematurely lysed. Due to sperm cell variability between individuals the protocol requires replicated tests. Within a simulated scenario there may be various concentrations and volumes of sperm when considering the male to female ratio, including the females stage of menstruation at the time of collection (58)(59). Considerations have to be made for sperm quality as various health factors may alter the quality of sperm including, previous abstinence, physical activity and personal nutrition (60)(61)(62). Swab variations can also influence sperm recovery due to getting entangled and retained within swab fibres (63)(64).

1.5.4 Nuclease-Based Approach

A nuclease-based approach was developed to decrease the amount of female DNA in the sample through DNase treatment after the initial lysis, rather than physical separation. Garvin et al.(39) demonstrated that the nuclease-based approach was successful after 61 hours' time-since-intercourse interval. Hudlow et al.(64) used buffers with two different concentrations of sodium hydroxide with the same protocol for the lysis of epithelial and sperm cells. Using this technique 96 swabs were extracted within 4 hours (64). The technique was better than differential lysis due to the lack of pipetting steps, reducing the loss of sperm (39)(64).

1.5.5 Alternative Approaches

Pressure cycling technology (PCT) aims to selectively lyse cells and release biomolecules through alternating cycles of hydrostatic pressure between ambient and ultra-high levels (36). Epithelial cells are selectively targeted among a forensic sample (intimate swab) and lysed with light hydrostatic pressure. Alkaline and PCT techniques were tested together. Samples with a female-to-male cell ratio of up to 5:1 can produce a clear male STR profile, with processing time reduced to 20 minutes (36). An extra PCT step and an adjustment to the sodium hydroxide concentrations resulted in the successful analysis of 100:1 female-to-male cell ratios. The inclusion of an immunomagnetic pre-treatment for epithelial cell detection resulted in a 200:1 female-to-male cell ratio analysis (36). Chen et al.(54) included two filtration-based methods to separate the spermatozoa from the epithelial cell lysate, it was concluded that the process is ineffective for sexual assault samples containing aged specimens (54).

The Nylon Membrane Brushing Separation Technique used physical separation following the digestion of epithelial cells (65). Cell debris and DNA migrate through the pores, whereas the undamaged sperm are captured by the nylon membrane (65). After the method was applied to 40 sexual assault samples, 37 samples (92.5%) produced a single-source male DNA profile. Compared to a conventional method, where 25 samples produced no male STR profile (36).

1.5.6 Kit-Based Methods

There are numerous kit-based methods which are also used among forensic DNA laboratories, including: i) Erase Sperm Isolation Kit (Erase) by Paternity Testing Corp; ii) Labs, Differex™ by Promega Corp. and iii) Sampletype i-sep® CL system by Biotype (36). Differex generates a male DNA fraction from a vaginal intimate swab eliminating wash steps. Instead of wash steps the sperm are pelleted through an organic buffer containing a higher density than the aqueous lysis buffer. This allows the sperm pellet to physically separate from the soluble remaining female DNA, which remains due to absorption to particles (cotton fibres) or

incomplete digestion of the victims DNA (36)(38). The protocol can be performed in 2 hours compared to differential extraction (24 hours) (36). According to Garvin et al.(38) the most challenging ratio of male-to-female cells were 1:20 which is higher than casework samples of 1:100, when the victims waits hours before reporting the crime and being examined (38). The separation solution produced issues such as droplets on the microscopy slide which were unable to dry. Valgren et al.(66) concluded in their study that the Differex™ method was not adaptable to forensic laboratories (66). In contrast, Vuichard et al.(67) compared Differex™ to differential extraction methods and concluded that Differex was the only method to result in a full male profile, with no contamination from epithelial cells (67).

The Erase kit is like the differential extraction methods as it uses Proteinase K/detergent lysis step for digesting the epithelial cells and eluting the sperm from the swab substrate. The pellet is then centrifuged, and supernatant removed (containing the victim's DNA). Instead of the wash step the sperm pellet is treated with a nuclease to remove any remaining DNA and the simultaneous inhibition of the nuclease (though removal of the two electrons required for nuclease activity), and lysis of sperm to generate a male DNA profile (38). Due to the lack of wash steps the protocol is faster and easier to perform than differential extraction. The female fraction from the Erase method may contain male DNA from non-sperm cells and tested using Y-STR profiling (38). Garvin et al (38) recommended although the Erase kit produced superior results, laboratories should also run a direct comparison with standard methods before use (38).

The Sampletype i-sep DL system is a mini spin-column-based method which only lets fluid pass through a filter during centrifugation. First the lysis of the epithelial cells is performed, then the lysed cells separated from the sperm cells. After numerous wash steps, in the same column the lysis of sperm cells is performed. The male DNA is collected in the final centrifugation step (36). The Sampletype i-sep® DL method resulted in the highest recovery of male DNA (64%) when compared with Differex™ (33%), Erase kit (8%) and differential lysis (62%) however, still insufficient (36)(40).

The traditional manual extraction method has been compared to the manual QIAGEN method and, QIAGEN QIAcube automated method (45). The manual QIAGEN extraction method initially began with cell lysis from the swab using 400 µL of stain extraction buffer and 15 µL proteinase K before overnight incubation at 56°C on a shaking platform. The lysate was separated using DNA IQ™ spin baskets for 5 minutes at 7500 x g. The sperm pellet was incubated at 56°C for 2 hours on a shaking platform, following the addition of phosphate buffered solution, QIAGEN proteinase K, DTT, and QIAGEN buffer solution. Sperm and non-sperm fractions were purified using the QIAamp® DNA Investigator kit. The traditional manual

extraction method used followed the same cell lysis protocol as the manual QIAGEN method however, used an organic extraction method for cell purification. The QIAGEN QIAcube automated method followed manufacturers recommendations regarding differential separation. The cells were lysed from the swabs using the "buccal swab spin protocol part A (lysis)" protocol. The sperm cell fraction was then lysed following the "differential wash protocol". Both sperm and non-sperm fractions were purified using the "buccal swab spin protocol part B (purification)" protocol with QIAamp® DNA Investigator kit reagents (45). The QIAcube method produced yielded more effective results as, none of the sperm fraction samples contained DNA content more than 1.2 times the estimated male DNA content. Compared to the manual QIAGEN and traditional methods as 72% and 30% of sperm fraction samples, respectfully, produced values which displayed a significant female contribution (>1.2:1 human:male ratios) (45). Human:male ratios in evidence samples which are greater than 1:1 are more likely to produce mixed STR profiles, resulting in a lengthier interpretation process (45)(68)(69)(70)(71).

1.5.7 Laser-Based Methods

Laser-based methods such as laser-capture microdissection (LCM) was proven as effective as isolating sperm cells through molecular separation. Research reported that a minimum of 30 isolated sperm are required to produce a clean male STR profile (72). LCM can be combined with sex-specific staining of sperm using fluorescence in situ hybridization (FISH), to enhance the sperm recovery (73). The fixing and staining of the specimen may result in male DNA degradation (74). Due to the intensive labour required for this LCM the method is not feasible for large laboratories (75).

An alternative laser-based approach to LCM is optical tweezers. Optical tweezers reduces the processing because the sperm cells are not required to be fixed, as they can be influenced in an aqueous solution (76). DNA analysis requires less than 60 spermatozoa to generate a full STR profile with the use of a QIAamp® DNA Investigator Kit and AmpFLSTR™ Identifier™ Plus PCR Amplification Kit (76). Female alleles were still detected with the use of this technology, though the experiments tests low ratios of female to male cells (76).

1.5.8 Microdevices

Microdevices have been utilized to isolate sperm from denser epithelial cells, through using the epithelial cells' adherence to the bottom of the device's inlet reservoir (36). To isolate sperm from dense epithelial cells, epithelial cell adherence is exploited as they adhere to the bottom of the glass device inlet reservoir, as vaginal epithelial cells are an adherent cell line (51). A settling time of 5 minutes is required before sperm are transported through an induced

flow to the outlet reservoir. This process had 25% sperm cell recovery and 1% epithelial cell recovery after 70 minutes of induced flow (51)(51).

An image-based technology using dielectrophoretic cages to move and trap fluorescent-labelled cells called DEPArray™ system by Menarini Silicon Biosystems, is another approach. This method yielded 100% purity however, only collected 15 to 64 spermatozoa per swab (50). More research is required into microdevices and the forensic applications to be viable for commercial use within a laboratory.

1.5.9 Antibody-Based Methods

Sperm cells can be captured from a sexual assault sample through immunomagnetic beads (55). The method uses antibodies against the testicular isoform of the angiotensin-converting enzyme (tACE) attached to the magnetic beads. Antibodies featuring differing proteins have been tested such as SP17 Polyclonal antibody, Intra Acrosomal Protein monoclonal antibody (SP10), and testicular isoform of the angiotensin-converting enzyme (tACE) (55)(56)

Sperm-binding antibodies require a high binding efficiency and specificity to sperm, and selectivity and sensitivity to the acrosome region of the sperm where nuclear DNA is stored (77). Antibodies which target the head of the spermatozoa are preferred as the tail and midpiece are the first anatomical characteristics to degrade (55).

For this study, α-Sperm Adhesion Molecule 1 (SPAM1), α-Sperm Acrosome Associated 1 (SPACA1), and α-Zona Pellucida Binding Protein (ZPBP) antibodies were tested.

The cross-reactivity of these selected antibodies with vaginal cells is currently unknown and was investigated through the study. Although infrequently used within forensic practices, immunomagnetic beads are capable of sperm enrichment and identification through sperm binding (78). The lowest reported cell concentration able to be detected is 10^3 spermatozoa, displaying the antibodies low sensitivity (78). The disadvantages to the method are the current lack of sensitivity, expensive reagents that are required and the sperm degradation after lengthy storage times or time since intercourse (TSI) intervals (78)(79).

Alternatively, other affinity-based methods such as aptamer binding could be used to isolate sperm. DNA molecules with altered affinity and base properties called slow off-rate modified aptamers (SOMAmers) have been used to isolate sperm cells (80). The method has produced similar sperm cell purification results to differential extraction however, the advantage is the application for automation in the future (80). Automation would allow less than two hours for rapid sperm isolation and DNA extraction, removing centrifugation steps (80). Further research is required into SOMAmer-based affinity method to conclude the usefulness in a forensic laboratory.

1.6 Antibodies

Antibodies are proteins produced by B cells with a Y-shaped morphology. When antigens are present antibodies will be produced by the body and bind to the antigen with a lock-and-key complex (81). Antibodies carryout numerous functions such as fixation, agglutination and neutralization and, protect the body from infections, viruses and pathogenic particles (82). Monoclonal and polyclonal antibodies are the two main types. Monoclonal antibodies can bind to a specific epitope on a corresponding antigen and are produced from a single B cell clone. In contrast, those produced from multiple B cell clones are polyclonal antibodies and can attach to various epitopes on the same antigen (82). α-sperm antibodies are employed in this study to determine the cross-reactivity against VK2/E6E7 (ATCC CRL-2616) cells and binding to spermatozoa. The sperm-specific antibodies have corresponding antigens located on the head of the sperm in the acrosomal region, which increases specificity. Antigens located in the acrosomal region of the sperm are important as the first segments of sperm degradation are the tail and midpiece (12). The specific primary antibodies researched in this study are α-SPAM1, α-SPACA1, and α-ZPBP1, as outlined in Table 4.

1.6.1 α-Sperm Adhesion Molecule 1 (SPAM1)

SPAM1 was previously known as the HYAL1 (Hyaluronidase 1) and HYA1 (Hyaluronidase 1) gene. The gene encodes an enzyme located on the acrosomal membrane and sperm surface called GPI-anchored enzyme. The hyaluronidase protein allows sperm to break through the oocyte cell layer, a receptor involved in sperm-zona pellucida adhesion (83). SPAM1 can also be detected in female genital tracts, and is transferred to the surface of the sperm when it resides in males or female genital tracts (84)(85).

A study that isolated sperm from cell mixtures used magnetic beads coupled with α-SPAM1 antibody (86). The immunomagnetic beads used were activated Dynabeads1M-270 Carboxylic Acid beads with 60µg of each antibody added. The sperm then underwent isolation, DNA extraction, amplification, and electrophoresis. Previous electron microscopy and immunogold labelling displayed the plasma membrane on the sperm head to be the location of SPAM1. SPAM1 was not however located on the sperm midpiece or tail (86). α-SPAM1 antibody was coated onto the bead with a covalent amide bond and incubated in a 1:1 mixture of epithelial and sperm cells at a concentration of 10^5 cells/mL. Once the beads were washed and resuspended, they were viewed through optical microscopy and scanning electron microscopy. The image displayed only sperm heads bound to the beads with no epithelial cell contamination (86). Epithelial cells were set at a concentration of 10^5/mL and mixtures were created with sperm at various concentrations from 10^2-10^5 cells/mL. Mixtures with sperm concentrations of 10^5 cells/mL and 10^4 cells/mL yielded a single-sourced DNA profile from the male fraction using capillary electrophoresis. Sperm cells at 10^2/mL concentration yielded no

single-sourced profile and therefore was the lower detection limit (86). The study measured the α-SPAM1 antibody against SP-10, a distintegrin and metal-loprotease 2 (ADAM2) and JNK-associated leucine zipper protein (JLP) and compared their effectiveness on the beads (86). α-SPAM1 yielded the best results at 10^3/mL sperm concentration as it was sensitive and successfully isolated sperm from a simulated mixed with epithelial cells. When compared to the differential lysis, the method resulted in 90% of mixed samples producing a single-sourced DNA profile. Whereas, differential lysis only resulted in one sample out of the 20 tested producing a single-sourced DNA profile (86). A challenge encountered throughout the study was the separation of sperm and epithelial cells. Even though no vaginal cells were visualized through microscopy, it was possible that fragments of female DNA from the lysis step could have been attached to the complex surfaces (86). A single-sourced STR profile of the male donor was produced from the DNase-treated immunomagnetic beads-sperm complexes (86). The study concluded that α-SPAM1 was sensitive to sperm cells and effectively excludes the female fraction of the sample (86).

1.6.2 α-Sperm Acrosome Associated 1 (SPACA1)

SPACA1 can be detected in all stages of acrosome development but is absent prior to the formation of the acrosome during spermatogenesis (85). SPACA1 is located on the inner acrosomal membrane of the whole acrosome and on the outer acrosomal membrane of the equatorial segment of mature sperm (85). The function of SPACA1 is to assist in sperm binding to the zona pellucida of oocytes. The antigen SPACA1 may also be linked to male immuno-infertility, as a result of a strong reaction of recombinant SPACA1 with serum taken from an α-sperm antibody-positive infertile man (85).

The cross-reactivity of SPACA1 to spermatozoa has been previously tested using flow cytometry analysis. α-SPACA1 was tested at 0.02 mg/ml with α-SPAM and was found that >30% of spermatozoa were binding to the cocktail of the two primary antibodies (87). Flow cytometry analysis was used to visualize the cells cross-reactivity using Alexa Fluor 488 secondary antibody to display the fluorescence. A-SPACA1 antibody still requires more research into its forensic applications using affinity-based methods.

1.6.3 α-zona pellucida binding protein 1 (ZPBP1)

ZPBP1 binds to the zona pellucida glycoprotein family with a calcium-dependent approach. Proacrosin competes with ZPBP1 during fertilization as it inhibits the binding of ZPBP1 to the zona pellucida (85). ZPBP1 is located on the inner acrosomal membrane coat of the whole acrosome and on the outer acrosomal membrane of the equatorial segment, similarly to SPACA1. The absence of ZPBP1 results in the disturbance of the Sertoli– spermatid junctions,

as it prevents proper acrosome compaction (85). Infertile men with abnormal morphology of the sperm head may have a mutation on the ZPBP1 gene (88).

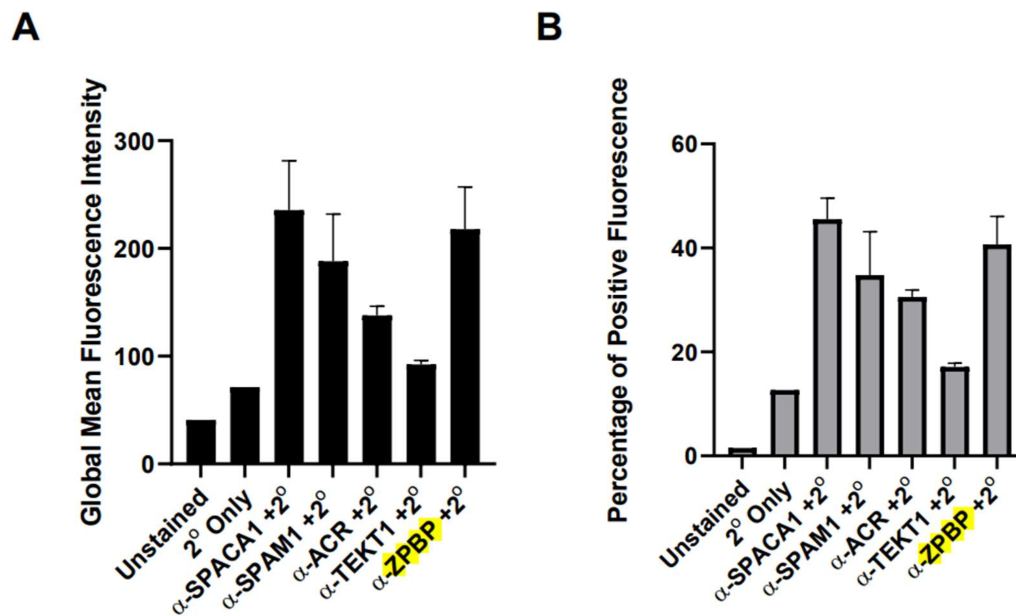

Figure 5: Screening of different primary antibodies for sperm binding under optimised flow cytometry conditions. Sperm was stained respectively with 0.01 mg/mL of each primary antibody: α-SPACA1, α-SPAM1, α-ACR, α-TEKT1 and α-ZPBP. A) Global mean fluorescence intensity (MFI). B) Percentage of positive cells. Data shown are mean and standard deviations from n=1 donor from a single experiment, performed in duplicate. 2°= secondary antibody (1:1200) (87).

ZPBP1 has been tested with sperm using flow cytometry and compared to other antibodies for effectiveness at sperm detection (87). α-ZPBP1, α-SPACA1, α-SPAM1, α-ACR, and α-TEKT1 were screened at a concentration of 0.01mg/mL. The results as demonstrated in Figure 5 show that, although ZPBP1 may not be the most efficient antibody to use there was still 41% of positive cells which bound to the antibody (87). The result suggests that ZPBP1 when used in conjunction with other antibodies can be useful in the detection of sperm cells however, on its own may not yield the most effective results. α-SPACA1 had the highest percentage of positive fluorescence with >40%. α-SPAM1 had <40% of positive florescence which was lowest out of the three.

Table 4: Sperm Specific Primary Antibodies

Primary Antibody	Clonality	Type	Host	Applications	Localization	Isotype	Catalogue Number
α-Sperm Adhesion Molecule 1 (SPAM1)	Polyclonal	Primary Antibody	Rabbit	Immunofluorescence	Acrosome	IgG	PA5-76062
α-Sperm Acrosome Associated 1 (SPACA1)	Polyclonal	Primary Antibody	Rabbit	Immunohistochemistry	Acrosome	IgG	PA5-55400
α-Zona Pellucida Binding Protein (ZPBP)	Polyclonal	Primary Antibody	Rabbit	Immunohistochemistry	Acrosome	IgG	PA5-21638

1.7 Flow Cytometry

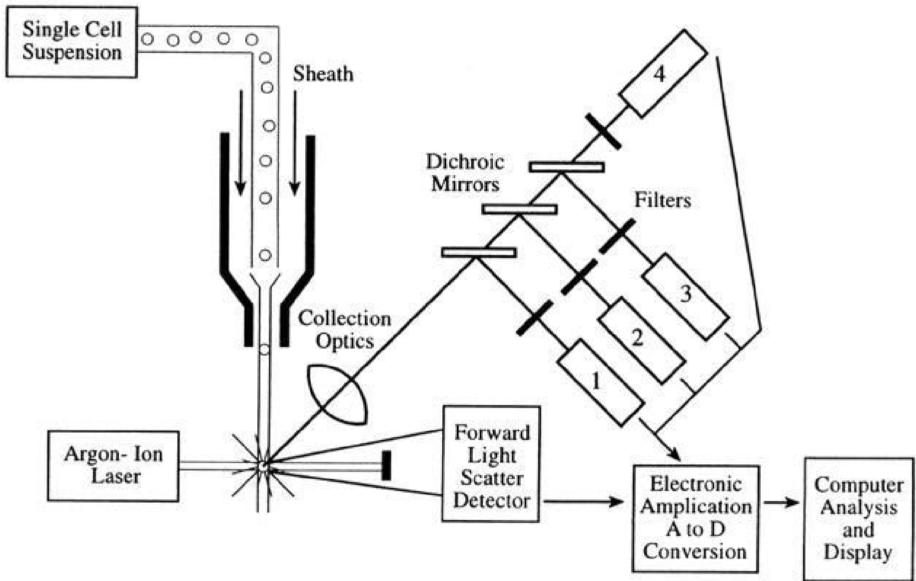

Figure 6: Diagram displaying the internal working of a flow cytometer. The sample in entered through the single cell suspension tube and transported through the machine using the fluidics system. The argon-ion laser, collection optics and forward light scatter detector are included in the optics system, before the data output onto a computer by the electronic system (89).

Flow cytometry was used throughout the study before beginning with the immunomagnetic beads due to the clearer visualization of antibodies binding to the sperm/epithelial cell population. It provides an inexpensive analysis of the cell cross-reactivity due to the consumption of less primary antibodies (to coat the beads) therefore, it's cheaper to run repeat tests (90)(91).

Flow cytometry can be used to identify and characterize immune cells through measuring cell size, surface receptors, and cell granularity (89). The flow cytometer works by monodispersing un-clumped cells in single file past a laser. Once the cells pass through the beam the cytometer will characterize the fluorescent and scattered light. The process of flow cytometry includes fluidics, optics and electronics (computer) as demonstrated in Figure 6 (89). The fluidics allows the cell suspension to pass through the machine while, the optics systems includes the optical filters, lenses and excitation light sources allowing alteration of wavelengths and generation of the photocurrent (89).

Flow cytometry has been used on sperm for reproductive purposes including sperm sexing, and evaluating sperm quality and DNA integrity (92)(93). Improvements have been developed for flow cytometry-based sperm sexing in sorting efficiency. Numerous factors have been tested to generate an efficient method for sperm sexing. Flow cytometric factors studied were

measurement resolutions, statistical and timing aspects, and cell orientation (92). Measurement resolution was tested to identify X- and Y- sperm which have only small differences in DNA content, by reducing background "noise" (92). Cell orientation is an important aspect of organizing sperm through flow cytometry as optical measurement artefacts can arise due to the shape of the sperm head (92). Further improvements have increased sperm sorted per second from 100-200 to 6000 sperm per second with optimized flow cytometry protocols (92).

Flow cytometry can also be used to evaluate the sperm quality in men. It has been applied to count sperm, and assess sperm viability, motility, apoptotic-like markers, acrosome reaction and DNA content (93). Two main flow cytometry-based assays have been explored, DNA stainability and sperm chromatin structure assay. DNA stainability works through DNA-specific dyes such as, DAPI, ethidium bromide/mithramycin and propidium iodide and the combination of chromatin packaging and flow cytometry techniques (93). The assay has been able to identify correlations between fertility capability and an increased abnormal sperm fraction (93). Sperm chromatin structure assays (SCSA) define sperm as normal or abnormal based on the amount of single-stranded DNA which it contains. SCSA parameters are used to detect breaks in the DNA strands (93). SCSA results are independent of sperm morphology, motility, and concentration, however, have been used toxicological, clinical and epidemiological studies. SCSA's have demonstrated a relationship between fertility potential and chromatin integrity within sperm. Studies suggest that when >30% sperm have altered chromatin, it can predict infertility (93)(94)(95).

1.7.1 Aims and Hypotheses of the thesis

Previous studies have aimed to achieve an optimized affinity-based approach for the isolation of sperm. Sperm-binding antibodies have been previously tested in isolated sperm samples however, this study aimed to optimize the use of three main antibodies α-SPAM1, α-SPACA1, and α-ZPBP for sperm detection in mixed sperm/vaginal cell samples.

The study aimed to achieve the following:

1. To determine the cross-reactivity of the α-sperm antibody cocktail to the VK2/E6E7 vaginal (ATCC® CRL2616™) cells using flow cytometry under the optimal conditions for sperm capture.
2. To determine the specificity and sensitivity of the α-sperm antibody cocktail for detecting sperm cells in a mock sexual assault swab sample using flow cytometry.

3. To evaluate the binding efficiency of the α-sperm antibody cocktail coated beads to the sperm cells from a mock sexual assault swab though immunomagnetic beading.

Hypotheses:

1. I hypothesised that the α-SPAM1, α-SPACA1, and α-ZPBP cocktail will bind to <30% of vaginal cells through flow cytometry.
2. I hypothesised that the α-SPAM1, α-SPACA1, and α-ZPBP cocktail will bind to >50% of the sperm cells from the mock sexual assault swab through flow cytometry.
3. I hypothesised that the α-SPAM1, α-SPACA1, and α-ZPBP cocktail coated beads will capture >50% of the sperm cells from the mock sexual assault swab through immunomagnetic bead selection.

2. Methods

2.1 Study Participants

The Murdoch University Ethics Committee approved the protocol for the collection of semen samples for the study (approval number 2017/128). Healthy adult volunteers were recruited using an electronic flyer and written consent was obtained. One self-declared healthy male participant over 20 years of age was used in this study.

2.2 Specimen Storage

Ejaculate was stored in 50mL specimen bottles and kept at 4°C until use. Sperm cells in each sample were counted and checked for viability and motility through trypan blue staining using light microscopy as per section 2.3. The neat ejaculate (semen and sperm) was diluted to $1x10^6$ cells/mL or $5x10^6$ cells/mL in FACS buffer before being stored on ice during the experiment.

2.3 Sperm Counting

The concentration of spermatozoa was calculated according to the World Health Organisation guidelines (96). The neat sperm was diluted 1 in 5 into FACS buffer and combined 1:1 with trypan blue (10µL cell suspension and10µL trypan blue). 10µl of the combined solution was loaded onto a haemocytometer. All 16 squares in the top corner of the grid of whole sperm (with a head and tail) were counted, as highlighted in Figure 7 (96). To calculate the concentration of spermatozoa per ml, the total number of sperm was multiplied by 10,000.

Numer of cells in a $1mm^2$ square (red) x 10^4 = No. cells/ml.

Figure 7: Haemocytometer grid to count sperm cells. The top corner of the grid outlined in red are the 16 squares used to calculate the concentration of sperm (97).

2.4 VK2/E6E7 (ATCC CRL-2616) Epithelial Cell Culture

An optimized protocol from the American Type Culture Collection (ATCC) guidelines was used to culture the VK2/E6E7 (ATCC CRL-2616) cells (33). Once the serum free growth medium was removed from the flask varying volumes (dependent of flask size) of 0.25% (w/v) trypsin-0.03% (w/v) EDTA were added to the flask to ensure the resuspension of the cells. The trypsin was neutralised with double the volume of DMEM:F12 medium, containing foetal bovine serum. The solution containing DMEM: F12 medium, trypsin, and cells in suspension was transferred to an appropriately sized centrifuge tube and centrifuged at 125xg for 5 minutes. The supernatant was removed, and cells resuspended in 1mL of serum free growth medium. A 10μl aliquot of cell suspension was added to 10μL of trypan blue stain and 10μ placed into a dual chamber counting slide. The cells were consistently counted using a TC20™ Automated Cell Counter throughout the course of the study. The remaining cells in the centrifuge tube were reseeded into a new flask for further cultures. Preparation of the cells for flow cytometry required a further centrifugation at 125xg for 5 minutes, supernatant removed and resuspension into FACS buffer.

2.5 FLOQSwab® saturation experiment

COPAN FLOQSwabs® (552C.80) were dipped into a small tray containing 10mL sterile water with the absorbent head in the water for 5 seconds. The swab head was then removed from the liquid, broken off the stick and placed into a spin basket located in a 1.5mL microfuge tube. Once sealed the tube was placed in a centrifuge at 4226 rpm (revolutions per minute) for 2 minutes. The dry swab head (in spin basket) was removed from the microfuge tube and the remaining volume of liquid was measured using an appropriate size pipette to evaluate the liquid holding capacity of the FLOQswabs.

2.6 Determination of epithelial cell binding to FLOQSwabs®

Once cells were split and counted according to section 2.4, the epithelial cells were resuspended in 1mL of serum free growth medium. Six FLOQSwabs® were separately dipped into the cell suspension for 5 seconds. As per the water experiment in 2.5, once removed, the swab head was broken off the stick and placed into a spin basket located in a 1.5mL microfuge tube. The swabs were centrifuged at 4226 rpm for 2 minutes. The dry swab head (in spin basket) was removed and the remaining liquid after centrifugation was measured and counted using 1:1 ratio with trypan blue stain and loaded into a dual chamber counting slide. The cells were counted using a brand TC20™ Automated Cell Counter.

2.7 Flow cytometry analysis

2.7.1 Primary Antibodies

Primary antibodies α-SPAM1 (PA5-76062), α-SPACA1 (PA5-55400) and α-ZPBP (PA5-21638) were used to target the surface antigens of spermatozoa and cross-reactivity of epithelial cells. α-SPAM1 and α-SPACA1 were diluted to 0.02 mg/mL whereas, α-ZPBP was set at 0.01 mg/mL as displayed in Table 5. The concentrations used, were optimized by a previous study.

Table 5: Primary and secondary antibody descriptions used in the study.

Antibody	Clonality/Type	Host/Isotype	Conjugate	Initial Concentration (mg/ml)	Final Concentration (mg/ml)	RRID	Supplier	Catalogue Number
α-Sperm Adhesion Molecule 1 (SPAM1)	Polyclonal / Primary Antibody	Rabbit / IgG	Unconjugated	1	0.02	AB_2719790	ThermoFisher Scientific	PA5-76062
α-Sperm Acrosome Associated 1 (SPACA1) Antibody	Polyclonal / Primary Antibody	Rabbit / IgG	Unconjugated	0.1	0.02	AB_2647765	ThermoFisher Scientific	PA5-55400
α-Zona Pellucida Binding Protein (ZPBP) Antibody	Polyclonal / Primary Antibody	Rabbit / IgG	Unconjugated	0.48	0.01	AB_11153689	ThermoFisher Scientific	PA5-21638
Alexa Fluor Plus 488 α-Rabbit IgG (H+L)	Polyclonal / Secondary Antibody	Goat / IgG	Alexa Fluor® Plus 488	2	0.07	AB_2633280	ThermoFisher Scientific	A32731

2.7.2 FACS buffer

FACS buffer was made by combining 1g Bovine serum albumin (BSA), with 100mL of Dulbecco's phosphate buffered saline (PBS). The BSA was measured and slowly combined with the PBS to dissolve. The solution was stored at 4°C until use. The buffer solution was used to dilute epithelial cells, sperm cells and antibodies for flow cytometry.

2.7.3 Optimisation of epithelial cell viability

Epithelial cell death was optimized for flow cytometry to produce a precise cell death control. Two cell killing methods were conducted- transillumination and rapid temperature fluctuations. Transillumination required the cells to be resuspended in 1mL of PBS after splitting as per section 2.4. Using a 24 well-plate, 300µl of the cell suspension was added to a well and placed onto the transilluminator for 15 minutes. Following the transilluminator the plate was placed into a 37°C incubator for cell recovery and death.

The rapid temperature fluctuations required the cells to be resuspended in 1mL of PBS following cell splitting, then cycled through a series of -20°C/60°C incubations for 15 minutes at each temperature. A total of two cycles were undertaken.

2.7.4 Flow cytometry assay

3ml FACS tubes were prepared with either 1×10^6 cells/mL or 5×10^6 cells/mL of sperm/epithelial cells, while keeping cell concentration consistent throughout the experiment. Cell types added to the tubes were dependent on the experiment. Epithelial or sperm cells were killed by adding 300µL of cells into a well of a 24 well plate and placed on a transilluminator for 15 minutes, before incubating at 37°C for a further 15 minutes. 10µL of 10% Normal Goat Serum (ThermoFisher Scientific), 15µL of FACS buffer or 5µL of each primary antibody working stock, and 1µL of live/dead viability dye were added. All samples were incubated at room temperature in the dark for 30 minutes. All samples were washed twice with 1mL of FACS buffer or PBS by centrifugation at 2000 rpm for 5 minutes. 50µL of FACS buffer was added to all samples and 1.25µL of 1/30 working stock of Alexa Fluor 488 secondary antibody were added to all appropriate samples. All samples were incubated on ice for 30 minutes in darkness to avoid light-bleaching. The wash step as mentioned above was repeated twice again, including centrifugation. 100µL of 4% paraformaldehyde was added to all tubes and incubated on ice for 15 minutes, to fix the cells. The wash step was repeated twice more before resuspending all cells in 500µL of FACS buffer and placing all samples on a vortex. Prior to analysis all samples were stored at 4°C in the dark.

2.7.5 Flow cytometry Analysis

The samples were run through a Canto™ II CA flow cytometer. The analysis on the flow cytometer required voltage adjustments for side-scatter, forward scatter, and Alexa Fluor 488

(for secondary antibody binding detection in stained samples). Linear and log voltages were explored and optimized to display both cell types on one graph. Multiple gating strategies were explored for data collection including a histogram to display positive cells. The Canto™ II CA had a stopping gate of 30,000 events, within the forward and side scatter gating strategy. The retrieved data was analysed using FlowJo™ version 8.0 software and was used in recording the global mean fluorescence intensity (MFI) and the percentage of positive cells.

3. Results

3.1 FLOQSwab® saturation experiment

To determine the maximum volume saturation of FLOQSwabs®, the protocol as per section 2.5 was conducted. Three centrifugation times were tested to optimize liquid extraction. The average liquid extraction when centrifuged for 1 minute was 140 µL as seen in Table 6. 1 minute 30 seconds and 2 minutes centrifugation produced 142 µL of water. Time and swab limitations resulted in only two tests conducted for 1 minute 30 seconds and two minutes centrifugation. Including the limitations, the optimal centrifugation time for a FLOQSwab® is 1 minute 30 seconds with an average saturation volume of 142 µL.

Table 6: The total saturation volumes (µL) of FLOQSwabs®. The swabs were dipped in a tray with 10mL of water for 5 seconds. Then placed in spin baskets within a 1.5mL Eppendorf tube and centrifuged at 4226 rpm for 1, 1 minute 30 seconds, and 2 minutes. Five swabs tested for 1 minute, and 2 swabs tested for each 1 minute 30 seconds and 2-minute centrifugation.

	1 minute	1 min 30 sec	2 minutes
Mean	140	142	142
Standard Deviation	13.99	4.51	5.51

3.2 Determination of epithelial cell binding to FLOQSwabs®

The binding of VK2 E6/E7 epithelial cells to FLOQSwabs was tested on 6 swabs as per section 2.6. Cells per swab was calculated using the cell recovery and the final volume eluted from the swab. Out of the six swabs the mean cell recovery per swab was 18,109 (+/- 2896.15) cells/swab. The lowest cell recovery was 12730 cells/swab and highest 22213 cells/swab (Table 7 and Figure 8). The mean percentage of cell recovery was 50.71% from the swab. The conditions throughout the experiment remained consistent however, fluctuations of cell recovery were seen among different swabs.

Table 7: Mean and standard deviation of vaginal cell recovery from FLOQSwabs®. Using the protocol as per section 2.6 to determine the vaginal cell recovery of saturated FLOQSwabs®. Number of cells per swab was calculated by converting the cells/mL to cells/μL and multiplying the cell recovery by the eluted volume.

Swab No	Initial Cell Concentration cells/mL	Final Cell Concentration cells/mL	Volume eluted (μL)	Cells eluted	Cells recovered per swab
1	397000	168000	97	229000	22213
2	397000	235000	113	162000	18306
3	397000	173000	83	224000	18592
4	397000	179000	91	218000	19838
5	397000	190000	82	207000	16974
6	397000	263000	95	134000	12730
Mean			94	195667	18109
Standard Deviation			10.36	35301.87	2896.15

Figure 8: Epithelial cell recovery (cells/swab) from FLOQSwabs®. Using the protocol as per section 2.6 to determine the vaginal cell recovery of saturated FLOQSwabs®. Number of cells per swab was calculated by converting the cells/mL to cells/μL and multiplying the cell recovery by the eluted volume. Conditions throughout the experiment remained consistent as swabs were saturated, centrifuged and counted using trypan blue staining.

3.3 Flow cytometry

3.3.1 Flow cytometry gating strategy

Forward scatter (FSC-A) allows discrimination of cells by size, through using the diffraction of the light to measure the diameter of the cell. Side scatter (SSC) however, measures the cells granularity through light reflecting from the laser interacting with the intracellular structures (98).

To assess the visualization of vaginal epithelial cells through flow cytometry an initial experiment was conducted, and the workflow presented in Figure 9. The initial experiments only included vaginal epithelial cells as seen in “A” in Figure 9. The gate drawn around the cellular population was labelled with the name of the cell type within the gate. Side scatter width and side scatter height was used to gate around the single cells to exclude any debris, doublets, or clumps as represented in “B” in Figure 9. Optimization methods to determine the fixable viability dyes effectiveness used a histogram of the dye (APC-Cy7) as seen in Figure 9 as “C”. A gate set close to 1.50 (a standard deviation) was set for the unstained control sample and compared to the stained samples to measure the percentage of positive cells. inclusivity was considered with the forward scatter area vs. side scatter area gate. The addition of anti-rabbit Alexa Fluro™ 488, α-SPAM1, α-SPACA1, and α-ZPBP used an anti-rabbit Alexa Fluro™ 488 histogram for the final gate to measure the percentage of positive cells that bound to the antibodies.

Figure 9: Flow cytometry gating strategy. Live vaginal epithelial cells were unstained with the absence of the fixable viability dye, anti-rabbit Alexa Fluro™ 488, and all primary antibodies. A) forward-scatter by side-scatter graph of unstained vaginal epithelial cells. B) side-scatter width by side-scatter height graph of unstained epithelial cells C) fixable viability dye (APC-Cy7) histogram with gate set at 1.56.

3.3.2 Optimisation of epithelial cell viability and live/dead dye

Epithelial cells were killed through transillumination, and freeze/thawing techniques as outlined in section 2.7.3. Transillumination of the cells resulted in 0% cell viability whereas, freeze/thaw resulted in 30% cell viability. The optimization resulted in cells being killed through transillumination for all proceeding experiments.

Epithelial cell viability was optimised to generate dead cell controls for further experiments. The optimization was conducted as per section 2.7.3. Data was recorded from three experiments which epithelial cells were run through the flow cytometer with a live unstained, live stained, dead unstained, and dead stained. The unstained samples were used as controls

for the efficiency of the fixable viability dye. No anti-rabbit Alexa Fluro™ 488 and primary antibodies were added to these experiments.

Figure 10 displays the percentage of positive cells which were stained by the live/dead fixability dye. The control was set by creating a 1.61 gate in the unstained sample histogram as displayed in Figure 10 section “C”. Both the live and dead controls had 99% of cells fluoresce with the stain, displaying that the fixable viability dye effectively stains the cells.

An experiment containing live and dead cells was conducted as per section 2.7.3. The experiment was aimed at ensuring effective killing of the epithelial cells and subsequently identifying the dead population using flow cytometry. The data present in Figure 11 was formulated from section “C” in Figure 11. The cells were gated in Figure 11 to separate the live and dead populations as best as possible however, the two populations overlapped into one another making them difficult to distinguish. Once the gate was made on one sample the analysis was copied to all samples within the experiment which were, live epithelial cells unstained, live epithelial cells stained and dead epithelial cells stained. Figure 11 demonstrates the population percentage of the dead cells within the third quadrant of the Figure 11 “C” gate. Figure 11 displays a higher percentage of dead cells in the dead control than the live control. 2.88% of the live control population was dead whereas, the dead cell population had 4.86% dead cells. The dead cell population has a low percentage however, higher than the live cell population. The limitation of the data was the cells overlapping.

Figure 12 demonstrates the back gating strategy for the fixable viability dye represented as APC-Cy7 in the graphs. Section “D” is a comparative histogram. The red histogram is the control sample with no viability dye added to the sample and a 1.61 gate added. The blue histogram represents dead cells with the addition of the viability dye which can be seen within the control gate resulting in a positive stain result. Dead cells were used for the comparison as the viability dye works to fluoresce the dead cells with red more than the live cells.

Section “E” in Figure 12 compares the live/dead-stained dead cell controls between the first three experiments. The aim of the experiments was to optimize the dead cell population for future experiments. The initial experiment as represented by the green population has a larger side-scatter spread, due to the voltage used on the flow cytometer. The green population when compared to the blue population has fewer dead cells with low granularity. The red population was the final optimization experiment and was conducted under optimal cell killing conditions by using a UV transilluminator. The final population of dead cells tested (red population) produced a big enough population for the cell death protocol to be used for future experiments.

Figure 10: **Percentage of positive cells for fixable viability stain (APC-Cy7).** A gate of 1.61 was set for the unstained sample and applied to the other samples within the experiment to measure positively stained cells.

Figure 11: **Comparison of live and dead epithelial cells.** The control are the live unstained cells to compare the difference when the stain is added to the cells. The data is the percentage of dead cell with in the third quadrant gate (presented as section "C" in figure 11).

	Sample Name	Subset Name	Count	Freq. of Parent
(blue)	Specimen_001_03 Dead Stained.fcs	Single Cells	20124	97.4
(red)	Specimen_001_01 Live Unstained.fcs	Single Cells	19819	95.9

	Sample Name	Subset Name	Count	Freq. of Parent
(red)	Specimen_001_03 Dead Stained.fcs	Single Cells	20124	97.4
(blue)	Specimen_001_04 Dead Stained.fcs	Single Cells	18274	95.8
(green)	Specimen_001_06 Dead Stained 60.fcs	Single Cells	11186	96.1

Figure 12: Back-gating strategy and comparative graphs. A) forward-scatter by side-scatter graph. B) side-scatter width by side-scatter height graph. C) fixable viability dye by side-scatter with four quadrant gates. D) viability dye effectiveness comparing live and dead stained samples. Histogram of fixable viability dye. E) Dead samples stained with fixable viability dye from three initial experiments, comparing populations.

3.3.3 Epithelial cell cross-reactivity with Secondary Antibody Alexa Fluor 488

Epithelial cells were stained with fixable viability dye and Alexa Fluor 488, including unstained controls. The flow cytometry protocol was followed as per section 2.7.4 however, in the place of the primary antibodies 15µL of FACS buffer was added to the tubes. All samples stained with secondary antibody had a consistent concentration and volume that was added (0.07mg/mL and 1.25µL respectfully).

The highest percentage of positive cells was 4.52% in the sample containing live epithelial cells stained with fixable viability dye and secondary antibody, as seen in Figure 13. The dead cells were gated separately to the live cells as the live cell gate resulted in 7% positive cells within the dead cell unstained sample. The gating strategy therefore resulted in the dead cell sample stained with anti-rabbit Alexa Fluro™ 488 to produce a higher percentage of positive cells then the control samples as 1.93% of cells were positive. The control samples both unstained and stained with fixable viability dye only produced consistent results with around 1.5% of positive cells. Dead cells stained with viability dye only resulted in an unexpected percentage of 0.95% of positive cells. The data retrieved for section "A" of Figure 13 was analysed through the gating strategy represented in Figure 14. Section "D" and "E" of Figure 13 represents a histogram of the live and dead cell samples stained with viability dye and anti-rabbit Alexa Fluro™ 488 shown in "A" of Figure 14.

The dead unstained sample and dead cell sample stained with both secondary antibody and viability dye had the highest MFI of positive cells with 142 and 144, respectfully. The two live cell samples without the presence of anti-rabbit Alexa Fluro™ 488 (controls) had consistent MFIs of 97.8 and 98.7. The dead cells stained with viability dye only produced an MFI of 127. The live cells stained with viability dye and anti-rabbit Alexa Fluro™ 488 had a lower MFI of positive cells with 111 (Figure 13 section "B").

Figure 14 section "C" reveals two clear populations of cells. The sample represented in the image contains live epithelial cells stained with viability dye and anti-rabbit Alexa Fluro™ 488 however, a dead population can be seen in quadrant 1. Few cells can be seen in quadrants 2 and 3 which were the cells that effectively bound to the secondary antibody (0.034% and 0.23% respectfully).

A

Percentage of Positivie Cells (%)

	Live Cells Unstained	Live Cells Stained with Viability Dye	Dead Cells Unstained	Dead Cells Stained with Viability Dye	Live Cells with Viability Dye + 2°	Dead Cells with Viability Dye + 2°

B

MFI of Positive Cells

	Live Cells Unstained	Live Cells Stained with Viability Dye	Dead Cells Unstained	Dead Cells Stained with Viability Dye	Live Cells with Viability Dye + 2°	Dead Cells with Viability Dye + 2°

Figure 13: The cross-reactivity of Alexa Fluoro 488 (secondary antibody) on epithelial cells. The live unstained data was gated at 1.60 and the dead unstained cells at 1.50 as the controls. A) Percentage of positive cells within the samples. B) Global mean fluorescence intensity (MFI). The analysis from the unstained samples were copied into the remaining data. The experiment was conducted as per section 2.7.4.

Figure 14: Cross-reactivity of Alexa Fluoro 488 on epithelial cells with back-gating strategy. The live unstained data was gated at 1.60 and the dead unstained cells at 1.50 as the controls. A) forward-scatter and side-scatter area. B) side-scatter width by side-scatter height, to determine granularity. C) Alexa Fluro 488 by fixable viability dye, to determine the staining fluorescence. D) Alexa Fluro 488 positive cell binding gate for live epithelial cells stained with fixable viability dye and secondary antibody. E) Alexa Fluro 488 positive cell binding gate for dead epithelial cells stained with fixable viability dye and secondary antibody.

3.3.4 Flow voltage optimization

The voltage used to visualize the cells on the flow cytometer had to be optimized to view the two cell types within the one graph. The flow protocol used throughout the experiment was as per section 2.7.4 without the presence of any antibodies and remained consistent throughout testing. Three voltages were tested including, linear epithelial cell, linear sperm cell, and mixed log voltages. The linear epithelial cell voltage consisted of FSC at 185V, SSC at 221V and APC-Cy7 at 360V. The linear sperm cell voltages consisted of FSC at 385V, SSC at 261V, and APC-Cy7 at 360V. The linear threshold remained consistent at 5,000 throughout the experiment. The log mixed cell voltages consisted of FSC at 75V, SSC at 161V and APC-Cy7 at 360V. The log threshold remained consistent at 1,000 throughout the experiment.

Section "A" and "B" in Figure 15 displays the difference in cell placement when the voltage was set at the epithelial linear voltage. The epithelial cells have a clear dense population in section "A" with the gate containing 96.2% of cells. Section "B" compares the sperm cell position to the epithelial cell position (VK2 cell gate). Due to the decrease in cell size of sperm compared to the epithelial cells the sperm were lower in the graph.

The epithelial cell population was not visible on the graph in section "C" when recorded at the linear sperm cell voltage. The cells displayed on the graph in section "C" may be cell debris or damaged cells as they are smaller than epithelial cells. The sperm cell population is visualized in section "D" and is gated with 59.6% cell population. The excess cells not gated within the graph may be cell debris or sperm tails which were present in the sample.

Due to issues with the linear voltages not presenting each cell type effectively, log voltages were considered. Section "E" of Figure 15 displays both epithelial and sperm cells positioned on the same graph effectively. 64.8% of the cell population were sperm cells and 22.2% of the population were epithelial cells. The limitation of the gates surrounding each cell type was that the gate had to be approximated, as there was no definitive split between the two populations. Epithelial cells may have been "bleeding" into the sperm cell gate and vice versa however, that is unknown from the FSC x SSC graph presented.

A

VK2 Cells

B

Sperm

C

VK2 Cells

D

Sperm Cells

E

VK2 and Sperm Cells

Figure 15: Optimization of flow cytometry voltages displaying epithelial and sperm cells. A) Live epithelial cells set at the linear epithelial voltage. B) Live sperm cells set at linear epithelial voltage. C) Live epithelial cells set at linear sperm voltage. D) Live sperm cells set at linear sperm cell voltage. E) Live mixed cell sample (epithelial and sperm cells) set at log voltage. No samples contained any primary or secondary antibodies.

3.3.5 Epithelial and sperm cell cross-reactivity with α-SPAM1, α-SPACA1, and α-ZPBP1 cocktail.

The cross-reactivity of the antibody cocktail with the use of anti-rabbit Alexa Fluro™ 488 for visualisation was determined using the protocol stated in section 2.7.4. The log voltages used consisently throughout the experiment were FSC – 75V, SSC – 161V, FITC – 490V, and APC-Cy7 – 440V. The voltage allowed for visualisation of both the epithelial and sperm cells, as displayed in Figure 16. 30,000 events were recorded for each sample, due to the amount of sample present in the tube. The experiment had a epithelial to sperm cell concentration ratio of 1:10.

The results from the experiment demonstrated cell overlapping as the sperm cell population spread upward into the epithelial quadrant and the epithelial cell bled down (Figure 16 section "B" and "C" respectfully). The mixed cell sample stained with the antibody cocktail, anti-rabbit Alexa Fluro™ 488 and viability dye had 12.7% positive sperm cells binding to the cocktail (Figure 16 section "D").

The highest frequency of sperm cells in quadrant 1 as displayed in Figure 16 is, the mixed sample with live cells stained with the antibody cocktail and viability dye with 3.71% of sperm cells. The highest frequency of epithelial cells in quadrant 2 was the epithelial cell sample stained with the antibody cocktail and viability dye with 3.31% of cells. The cells in quadrant 1 are assumed to be sperm cells which have bound to the antibody cocktail and, quadrant 2 are the epithelial cells which are assumed to have bound. The limitation of the gating strategy presented in Figure 16 is that there were no definitive spaces in all the cell populations therefore, it is possible for some cells to "bleed" into other quadrants.

The global MFI remained consistent throughout both cell types represented in section "B" and "D". Unstained live sperm cells produced the lowest global MFI out of all of the samples at 2233.

The control samples for the percentage of positive cells acted as expected as they were the lowest percentages in their relative quadrants. The sperm cell sample stained with the antibody cocktail, viability dye and anti-rabbit Alexa Fluro™ 488 had the highest percentage of positive cells at 22.3% in quadrant three. Quadrant four had high percentages of positive cells in the epithelial cell control samples. The increased fluorescence in the unstained samples suggest the vaginal epithelial cells have high autoflorescence. The epithelial sample stained with the antibody cocktail, viability stain, and anti-rabbit Alexa Fluro™ 488 displayed 31.6% positive cells however, due to the unstained results this may be due to autoflorescence

(Figure 17). It is unknown in this experiment how the epithelial cells reacted to anti-rabbit Alexa Fluro™ 488 only, as there was no control sample to analyse.

Figure 16: Cross-reactivity of sperm and epithelial cells to the α-SPAM1, α-SPACA1, and α-ZPBP1 antibody cocktail using anti-rabbit Alexa Fluro™ 488 for visualization. A) Secondary antibody by forward-scatter of the mixed sample stained with the antibody cocktail, viability dye and anti-rabbit Alexa Fluro™ 488. B) Secondary antibody by forward-scatter of the sperm cell sample stained with the antibody cocktail, viability dye and anti-rabbit Alexa Fluro™ 488. C) Secondary antibody by forward-scatter of the epithelial sample stained with the antibody cocktail, viability dye and anti-rabbit Alexa Fluro™ 488. D) Alexa Fluro 488 histogram of positive cells in the mixed sample stained with the antibody cocktail, viability dye and anti-rabbit Alexa Fluro™ 488. Data collected from quadrant four. E) Alexa Fluro 488 histogram of positive cells in the mixed sample stained with the antibody cocktail, viability dye and anti-rabbit Alexa Fluro™ 488. Data collected from quadrant three.

A

Cell Frequency (%)

4
3.5
3
2.5
2
1.5
1
0.5
0

Sperm Cell Alive Unstained
Sperm Cell Alive + APC-Cy7
Sperm Cell Alive APC-Cy7 + FITC (Secondary Only)
Sperm Cell Alive APC-Cy7 + FITC (All)
Sperm + VK2 Cells Alive APC-Cy7 + FITC (All)
Sperm + VK2 Cells Live APC-Cy7 + FITC (SPACA)
Sperm + VK2 Cells Dead APC-Cy7 + FITC (All)

B

Global MFI

6000
5000
4000
3000
2000
1000
0

Sperm Cell Alive Unstained
Sperm Cell Alive + APC-Cy7
Sperm Cell Alive APC-Cy7 + FITC (Secondary Only)
Sperm Cell Alive APC-Cy7 + FITC (All)
Sperm + VK2 Cells Alive APC-Cy7 + FITC (All)
Sperm + VK2 Cells Live APC-Cy7 + FITC (SPACA)
Sperm + VK2 Cells Dead APC-Cy7 + FITC (All)

C

Cell Frequency (%)

3.5
3
2.5
2
1.5
1
0.5
0

VK2 Cell Alive Unstained
VK2 Cell Dead Unstained
VK2 Cell Live + APC-Cy7
VK2 Cell Dead + APC-Cy7
VK2 Cell Alive APC-Cy7 + FITC (All)
Sperm + VK2 Cells Alive APC-Cy7 + FITC (All)
Sperm + VK2 Cells Live APC-Cy7 + FITC (SPACA)
Sperm + VK2 Cells Dead APC-Cy7 + FITC (All)

D

Global MFI

50000
45000
40000
35000
30000
25000
20000
15000
10000
5000
0

VK2 Cell Alive Unstained
VK2 Cell Dead Unstained
VK2 Cell Live + APC-Cy7
VK2 Cell Dead + APC-Cy7
VK2 Cell Alive APC-Cy7 + FITC (All)
Sperm + VK2 Cells Alive APC-Cy7 + FITC (All)
Sperm + VK2 Cells Live APC-Cy7 + FITC (SPACA)
Sperm + VK2 Cells Dead APC-Cy7 + FITC (All)

E

Positive Cells (%)

25
20
15
10
5
0

VK2 Cell Alive Unstained | VK2 Cell Dead Unstained | VK2 Cell Live + APC-Cy7 | VK2 Cell Dead + APC-Cy7 | Sperm Cell Alive Unstained | Sperm Cell Alive + APC-Cy7 | Sperm Cell Alive APC-Cy7 + FITC (Secondary Only) | Sperm Cell Alive APC-Cy7 + FITC (All) | VK2 Cell Alive APC-Cy7 + FITC (All) | Sperm + VK2 Cells Alive APC-Cy7 + FITC (All) | Sperm + VK2 Cells Live APC-Cy7 + FITC (SPACA) | Sperm + VK2 Cells Dead APC-Cy7 + FITC (All)

F

Positive Cells (%)

40
35
30
25
20
15
10
5
0

VK2 Cell Alive Unstained | VK2 Cell Dead Unstained | VK2 Cell Live + APC-Cy7 | VK2 Cell Dead + APC-Cy7 | Sperm Cell Alive Unstained | Sperm Cell Alive + APC-Cy7 | Sperm Cell Alive APC-Cy7 + FITC (Secondary Only) | Sperm Cell Alive APC-Cy7 + FITC (All) | VK2 Cell Alive APC-Cy7 + FITC (All) | Sperm + VK2 Cells Alive APC-Cy7 + FITC (All) | Sperm + VK2 Cells Live APC-Cy7 + FITC (SPACA) | Sperm + VK2 Cells Dead APC-Cy7 + FITC (All)

Figure 17: The binding-efficiency of sperm and epithelial cells to α-SPAM1, α-SPACA1, and α-ZPBP1 antibody cocktail using anti-rabbit Alexa Fluro™ 488 for visualization. Flow cytometry protocol as per section 2.7.4 remained consistent throughout the experiment. A) Cell frequency percentage of sperm cells (quadrant one). B) Global MFI of sperm cells. C) Cell frequency percentage of epithelial cells (quadrant two). D) Global MFI of epithelial cells. E) Percentage of positive cells from quadrant three analysis. Unstained sample was set at 1.54. F) Percentage of positive cells from quadrant four. The flow cytometer ran 30,000 events from each sample consistently.

4. Discussion

4.1 Epithelial cell binding and saturation of FLOQSwab®

Volume saturation of FLOQSwabs® was not stated in the manufacturer specifications however, data from this thesis concluded the average saturation volume is approximately 141.5μL. The importance is to confirm the maximum volume of liquid the swab can hold and may be used to calculate the swab saturation point of sperm and vaginal cells in the future. The mean vaginal epithelial cell recovery was 18,109 (+/- 2896.15) cells/swab, with fluctuating data from the other swabs tested. The fluctuations could have been due to multiple factors including but not limited to, time cells remained on the swab before elusion, swab fibre interactions with the cells, and centrifugation speeds. Volume saturation of FLOQSwabs® was not stated on the manufacturers specifications nor has it been discussed in any published articles.

Cells were spun at the low speed of 4226 rpm however, the end of the FLOQSwabs® still appeared dry after centrifugation. The speed was necessary to maintain the sperm/epithelial cells integrity and ensure no cells were compromised during centrifugation. A study from the Journal of Extracellular Vesicles states that high-speed centrifugation can compromise cell integrity and induce aggregation, as cells were spun at speeds up to 20,000 g (99).

4.2 Optimisation of epithelial cell viability and live/dead dye

Optimization of vaginal cell viability used flow cytometry to determine whether a vaginal cell population was dead. Two cell killing protocols were tested as per section 2.7.3, temperature fluctuations and 15 minutes on a transilluminator. Both protocols required the vaginal epithelial cells to be placed in an incubator for 15 minutes after the initial killing step. The incubation time allows for the cells to respond to the harsh treatment. The transilluminator proved the most effective method with 0% viability after the treatment, resulting in the epithelial cells responding to the UV treatment. It can be hypothesized that the temperature fluctuations were ineffective for the vaginal epithelial cells as temperatures around -20°C can slow down cell functions and not kill the cell itself (20).

Flow cytometry testing revealed a dead population did arise after optimization of the protocol as the dead control produced 4.9% dead epithelial cells in the population compared to 2.9% in the live cell population. The workflow (gating strategy) used to process the data displayed in Figure 12 demonstrates an overlap of the live and dead cell population. It is important to consider researcher error when gating the live/dead populations however, future studies may work to optimize the flow protocol to create two separate distinct populations.

4.3 Epithelial cell cross-reactivity with Secondary Antibody Alexa Fluor 488

Vaginal epithelial cells were stained with secondary antibody Alexa Fluor to determine the cross-reactivity of the cells with the secondary antibody. The highest percentage of positive cells were the live cells stained with the viability dye and Alexa Fluro with 4.5% of positive cells. The interactions between the epithelial cells and the secondary antibody could have been due to the "stickiness" of the cell resulting in the epithelial cell binding to secondary antibody directly. Some receptors on the epithelial cells may also have an interaction with the secondary antibody used therefore, other secondary antibodies (PE-conjugated secondary antibodies) could be explored in future studies. Results from this experiment were obtained using a linear voltage flow graph as only one cell type was under review.

4.4 Optimisation of flow voltage and epithelial/sperm cell cross-reactivity with α-SPAM1, α-SPACA1, and α-ZPBP1 cocktail.

Epithelial cells are large when compared to spermatozoa. The size of the epithelial and sperm cells is demonstrated in Figure 15. The epithelial cells when run through flow analysis under optimal epithelial cell voltage are seen in the top right corner of the graph whereas, the sperm cells are positioned lower and to the left of the epithelial cell population. It is also important to note in section "B" of Figure 15 there are still sperm cells present within the epithelial cell gate demonstrating both cell types may overlap into the other cell population. Within section "C" using the optimal sperm cell voltages the epithelial cells are out of the graph and therefore are too "big" to be present within that scale. The optimal log voltages were set as per section 3.3.4 however, the overlap of each cell type into the opposing population must be considered. Figure 15 displays two gates set, one for the sperm cell population and the other the epithelial cells. It is important to consider that each gate may not solely contain the cell they're labelled with due to the cells overlapping in each population. Future studies may work to optimize the flow protocol or voltage optimization further to ensure each cell population are displayed separately on the flow graph with no overlapping.

To identify male perpetrators of a sexual assault, DNA profiles from spermatozoa need to be produced. High abundance of epithelial cells compared to spermatozoa on sexual assault swabs means new methods to enrich and isolate the sperm are urgently required (100). α-sperm antibodies such as α-SPAM1, α-SPACA1, and α-ZPBP1 target the corresponding antigens located on the acrosomal region of the sperm (12). These capabilities were utilized within this study to assess the specificity and sensitivity of the antibodies to sperm compared to epithelial cells using flow cytometry analysis. The study also aimed to assess the epithelial cell loss from a FLOQSwab® under laboratory conditions as stated in section 2.6. Three key findings from this study were:

1. The average epithelial cell recovery from a FLOQSwab® was 18,109 (+/- 2896.15) cells/swab.
2. The sperm cell sample stained with the antibody cocktail, viability dye and anti-rabbit Alexa Fluro™ 488 had the highest percentage of positive cell binding at 22.3%.
3. The epithelial cells had a higher autofloresce than expected (>30% of positive unstained cells), as displayed in Figure 16.

The data recorded in this thesis does not support the hypothesis that the α-SPAM1, α-SPACA1, and α-ZPBP cocktail will bind to <30% of vaginal cells through flow cytometry. Figure 16 displays >30% positive epithelial cell binding to the antibody cocktail. The controls also displayed >30% positive cells. It can be hypothesized that cellular autofluorescence of the epithelial cells may be causing the high percentage of positive cells within the controls, which can be explored within future studies. The viability dye and secondary antibody only control among the epithelial cells was missing due to researcher error. It can be hypothesized that, the increase in florescence could have been due to secondary antibody binding.

The data does not support the hypothesis that the α-SPAM1, α-SPACA1, and α-ZPBP cocktail will bind to >50% of the sperm cells from the mock sexual assault swab through flow cytometry. The highest percentage of sperm cell binding to the antibody cocktail was 22.3%. This may be due to epithelial cell interference and binding of the antibodies (54). Further studies are required to optimize cell specificity and ensure that the percentage of sperm binding to the antibody cocktail is >50% and epithelial cell binding is <30%.

A-SPAM1 antibody is also featured in a study which isolated sperm using α-SPAM1 coated immunomagnetic beads. The lowest concentration of sperm which was successfully isolated using α-SPAM1 was 10^3 cells/mL (86). This can be compared to 10^6 cell/mL of sperm that was used throughout this thesis. 90% of mixed samples produced a single-sourced DNA profile (86). The study found that during the lysis of the mixed samples fragments of female DNA may have remained within the sample for STR profiling (86). The use of α-SPACA1, and α-ZPBP1 antibodies for sperm extraction and isolation have not yet been applied to forensic methods

4.5 Limitations

Numerous limitations throughout the research period of study hindered the production of flow cytometric results. The SARS-Cov-2 pandemic delayed the α-SPAM1, α-SPACA1, α-ZPBP antibodies, and other reagents used throughout the experimentation from arriving at expected timeframes. The accelerated timeframe which the study was conducted resulted in less optimization and results than initially expected. Only one log voltage experiment was able to

be conducted including both sperm and epithelial cells, which did not include a control for epithelial cells stained with viability dye and anti-rabbit Alexa Fluro™ 488 only. The timeframe did not allow for the immunomagnetic bead testing and therefore, the hypothesis cannot be commented on.

Only one sperm donor was used throughout the study therefore, the data does not include variations which may occur among different sperm donors.

4.6 Conclusion

In summary, this study assessed the cross-reactivity of sperm and vaginal epithelial cells with a α-SPAM1, α-SPACA1, and α-ZPBP1 antibody cocktail. Optimization of epithelial cell death resulted in the use of a transilluminator for 15 minutes prior to 15 minutes incubation in 37°C, to ensure an effective dead population control. Using the linear voltage, the epithelial cells stained with anti-rabbit Alexa Fluro™ 488 and viability dye displayed <5% of positive cells. The highest percentage was 4.5% when live epithelial cells were stained with Alexa Fluro and viability dye only. The flow cytometry protocol was then optimized for better visualization.

To visualize the data from both sperm and epithelial cells in one graph, a log voltage was explored. Once the flow cytometry protocol was optimized the sperm and epithelial cells were combined with the antibody cocktail both separately and mixed at a 1:10 ratio. The results concluded that >20% sperm cells bound to the cocktail whereas, >30% epithelial cells bound to the cocktail (Figure 16). The unstained control epithelial cells had >25% of positive cell binding which may be the result of cell autofluorescence. Lacking the epithelial cell stained with Alexa Fluro only control, the direct binding of the secondary antibody to the cell is unknown.

A limitation of the study was the use of a single sperm donor resulting in no comparisons or variations in sperm data. Time limitations resulted in no repeat experiments or optimization of epithelial antibody binding however, can be explored through future studies. Findings from this thesis can be used as a base for future sperm isolation experiments involving the α-SPAM1, α-SPACA1, and α-ZPBP1 antibody cocktail. Immunomagnetic bead experiments can be used to confirm cell specificity in the isolation of sperm and percentage of DNA recovery can be calculated. The optimized protocol could be tested in a clinical setting using mock sexual assault swabs post-intercourse.

Overall, this study has provided useful information regarding sperm and vaginal cell cross-reactivity with a α-SPAM1, α-SPACA1, and α-ZPBP1 antibody cocktail. This study provides information that could be useful for future research in expanding the knowledge of forensic science.

5. References

1. Australian Institute of Health and Welfare. Sexual assault in Australia. Canberra; 2020.
2. Types of Sexual Assault - Women's & Gender Center [Internet]. [cited 2021 May 14]. Available from: https://www.marshall.edu/wcenter/sexual-assault/types-of-sexual-assault/
3. Clark C, Turiello R, Cotton R, Landers JP. Analytical approaches to differential extraction for sexual assault evidence. Vol. 1141, Analytica Chimica Acta. Elsevier B.V.; 2021. p. 230–45.
4. Terms and Phrases to Avoid* * Used and modified with permission by AHS Human Resources from the Guide To Creating Safe and Welcoming Places for Sexual & Gender Diverse (LGBTQ*) People (2016).
5. CDC. The National Intimate Partner and Sexual Violence Survey: 2015 Data Brief — Updated Release.
6. Bove G Del, Stermac L, Bainbridge D. Comparisons of Sexual Assault Among Older and Younger Women. J Elder Abuse Negl [Internet]. 2008 [cited 2021 May 28];17(3):1–18. Available from: https://www.tandfonline.com/action/journalInformation?journalCode=wean20
7. Stoltenborgh M, van IJzendoorn MH, Euser EM, Bakermans-Kranenburg MJ. A global perspective on child sexual abuse: Meta-analysis of prevalence around the world. Child Maltreat [Internet]. 2011 May [cited 2021 May 28];16(2):79–101. Available from: https://pubmed.ncbi.nlm.nih.gov/21511741/
8. Koss MP, Heise L, Russo NF. THE GLOBAL HEALTH BURDEN OF RAPE. Vol. 18, Psychology of Women Quarterly. 1994.
9. Muldoon KA, Denize KM, Talarico R, Fell DB, Sobiesiak A, Heimerl M, et al. COVID-19 pandemic and violence: rising risks and decreasing urgent care-seeking for sexual assault and domestic violence survivors. BMC Med [Internet]. 2021 [cited 2021 May 28];19(20). Available from: https://doi.org/10.1186/s12916-020-01897-z
10. Khoshnood A, Ohlsson H, Sundquist J, Sundquist K. A Comparison between Indoor and Outdoor Rape Suspects in Sweden. 2021 [cited 2021 May 28]; Available from: https://doi.org/10.1080/01639625.2021.1891844
11. Riggs N, Houry D, Long G, Markovchick V, Feldhaus KM. Analysis of 1,076 cases of sexual assault. Ann Emerg Med. 2000 Apr 1;35(4):358–62.
12. Rogers C. (PDF) The prevalence of intact spermatozoa on intimate smear and extract slides: a retrospective case review and re-evaluation of time since intercourse estimation [Internet]. Boston University; 2014 [cited 2021 May 20]. Available from: https://www.researchgate.net/publication/332410415_The_prevalence_of_intact_spermatozoa_on_intimate_smear_and_extract_slides_a_retrospective_case_review_and_re-evaluation_of_time_since_intercourse_estimation
13. The Royal College of Pathologists Australia. Evidence Based Forensic Sampling Standards [Internet]. 2018 [cited 2021 Jun 21]. Available from: https://www.rcpa.edu.au/getattachment/a83318be-18cf-42f9-9332-7856856131f1/Evidence-Based-Forensic-Sampling-Standards.aspx
14. Guidelines for medico-legal care for victims of sexual violence: 5 Forensic specimens.
15. Freedman E. Clinical Management of patients presenting following a sexual assault. Aust J Gen Pract. 2020;49(7).
16. Government of Western Australia North Metropolitan Health Service King Edward Memorial Hospital. Sexual Assault Resource Centre (SARC) [Internet]. 2017 [cited 2021 Jun 22]. Available from: https://kemh.health.wa.gov.au/Our-services/Service-directory/SARC
17. Brownlow RJ, Dagnall KE, Ames CE. A Comparison of DNA Collection and Retrieval from Two Swab Types (Cotton and Nylon Flocked Swab) when Processed Using Three QIAGEN Extraction Methods. J Forensic Sci [Internet]. 2012 May 1 [cited 2021 Dec 9];57(3):713–7. Available from: https://onlinelibrary.wiley.com/doi/full/10.1111/j.1556-4029.2011.02022.x
18. Daley P, Castriciano S, Chernesky M, Smieja M. Comparison of flocked and rayon swabs for collection of respiratory epithelial cells from uninfected volunteers and symptomatic patients. J Clin Microbiol [Internet]. 2006 Jun [cited 2021 Dec 9];44(6):2265–7. Available from: https://pubmed.ncbi.nlm.nih.gov/16757636/

19. Bruijns BB, Tiggelaar RM, Gardeniers H. The Extraction and Recovery Efficiency of Pure DNA for Different Types of Swabs. J Forensic Sci [Internet]. 2018 Sep 1 [cited 2021 Dec 9];63(5):1492–9. Available from: https://pubmed.ncbi.nlm.nih.gov/29890011/

20. Benschop CCG, Wiebosch DC, Kloosterman AD, Sijen T. Post-coital vaginal sampling with nylon flocked swabs improves DNA typing. Forensic Sci Int Genet [Internet]. 2010 Feb [cited 2021 Dec 9];4(2):115–21. Available from: https://pubmed.ncbi.nlm.nih.gov/20129470/

21. FLOQSwabs | COPAN Diagnostics Inc. [Internet]. [cited 2021 Dec 9]. Available from: https://www.copanusa.com/sample-collection-transport-processing/floqswabs/

22. Welch J, Cybulska B, Forster G, Lacey H, Rogstad K. Draft UK National Guidelines on The Management of Adult and Adolescent Complainants of Sexual Assault 2010 Draft UK National Guidelines on The Management of Adult and Adolescent Complainants of Sexual Assault 2010 Clinical Effectiveness Group British Association for Sexual Health and HIV [Internet]. 2015 [cited 2021 Jun 22]. Available from: https://www.researchgate.net/publication/265204461

23. Gaensslen R E HCL. Sexual Assault Evidence: National Assessment and Guidebook | Office of Justice Programs [Internet]. 2001 [cited 2021 Jul 19]. p. 1–119. Available from: https://www.ojp.gov/ncjrs/virtual-library/abstracts/sexual-assault-evidence-national-assessment-and-guidebook

24. Mortimer D. The functional anatomy of the human spermatozoon: relating ultrastructure and function. Mol Hum Reprod [Internet]. 2018 Dec 1 [cited 2021 Jul 2];24(12):567–92. Available from: https://academic.oup.com/molehr/article/24/12/567/5095621

25. Abou-Haila A, Tulsiani DRP. Mammalian sperm acrosome: Formation, contents, and function. Arch Biochem Biophys. 2000 Jul 15;379(2):173–82.

26. Bhutani K, Stansifer K, Ticau S, Bojic L, Villani AC, Slisz J, et al. Widespread haploid-biased gene expression enables sperm-level natural selection. Science (80-). 2021 Mar 5;371(6533).

27. Austin C. Haploid [Internet]. National Human Genome Research Institute. [cited 2022 Mar 3]. Available from: https://www.genome.gov/genetics-glossary/haploid

28. Martin-DeLeon PA. Epididymal SPAM1 and its impact on sperm function. Mol Cell Endocrinol. 2006 May 16;250(1–2):114–21.

29. Zhou CJ, Wu SN, Shen JP, Wang DH, Kong XW, Lu A, et al. The beneficial effects of cumulus cells and oocyte-cumulus cell gap junctions depends on oocyte maturation and fertilization methods in mice. PeerJ [Internet]. 2016 [cited 2021 Jul 2];2016(3). Available from: /pmc/articles/PMC4782716/

30. UniProt Consortium. SPACA1 - Sperm acrosome membrane-associated protein 1 precursor - Homo sapiens (Human) - SPACA1 gene & protein [Internet]. [cited 2021 Jul 2]. Available from: https://www.uniprot.org/uniprot/Q9HBV2

31. MBInfo. What is exocytosis? [Internet]. 2018 [cited 2021 Jul 2]. Available from: https://www.mechanobio.info/what-is-the-plasma-membrane/what-is-membrane-trafficking/what-is-exocytosis/

32. Classification of Vaginal Epithelial Cells [Internet]. [cited 2021 Dec 9]. Available from: http://www.vivo.colostate.edu/hbooks/pathphys/reprod/vc/cells.html

33. VK2/E6E7 | ATCC [Internet]. 2021 [cited 2021 Nov 17]. Available from: https://www.atcc.org/products/crl-2616#detailed-product-information

34. Lander ES, Linton LM, Birren B, Nusbaum C, Zody MC, Baldwin J, et al. Initial sequencing and analysis of the human genome. Nature [Internet]. 2001 Feb 15 [cited 2021 Dec 9];409(6822):860–921. Available from: https://pubmed.ncbi.nlm.nih.gov/11237011/

35. Wyner N, Barash M, McNevin D. Forensic Autosomal Short Tandem Repeats and Their Potential Association With Phenotype. Front Genet. 2020 Aug 6;11:884.

36. Chapman BRB, Blackwell SJ, Müller LH. Forensic Techniques for the Isolation of Spermatozoa from Sexual Assault Samples-A Review. Forensic Sci Rev [Internet]. 2020 [cited 2021 Jun 21];32:105–16. Available from: https://www-proquest-com.libproxy.murdoch.edu.au/docview/2431032733?accountid=12629&pq-origsite=summon

37. Kumar N, Maitray A, Gupta R, Sharma D, SK S. Importance of Y- STR profiling in sexual assault cases with mixed DNA profile. Int J Mol Biol. 2018 Feb 27;3(1).

38. Garvin AM, Fischer A, Schnee-Griese J, Jelinski A, Bottinelli M, Soldati G, et al. Isolating DNA from

sexual assault cases: a comparison of standard methods with a nuclease-based approach. Investig Genet 2012 31 [Internet]. 2012 Dec 4 [cited 2021 Jul 19];3(1):1–10. Available from: https://investigativegenetics.biomedcentral.com/articles/10.1186/2041-2223-3-25

39. Garvin A, Bottinelli M, Gola M, Conti A, Soldati G. DNA preparation from sexual assault cases by selective degradation of contaminating DNA from the victim. J Forensic Sci [Internet]. 2009 Nov [cited 2021 Jul 17];54(6):1297–303. Available from: https://pubmed.ncbi.nlm.nih.gov/19818111/

40. Gill P, Lygo JE, Fowler SJ, Werrett DJ. An evaluation of DNA fingerprinting for forensic purposes. Electrophoresis [Internet]. 1987 Jan 1 [cited 2021 Jul 7];8(1):38–44. Available from: https://analyticalsciencejournals.onlinelibrary.wiley.com/doi/full/10.1002/elps.1150080109

41. Wiegand P, Schürenkamp M, Schütte U. DNA extraction from mixtures of body fluid using mild preferential lysis. Int J Legal Med [Internet]. 1992 Nov [cited 2021 Jul 7];104(6):359–60. Available from: https://link.springer.com/article/10.1007/BF01369558

42. Bogas V, Bento AM, Serra A, Brito P, Lopes V, Sampaio L, et al. Validation of sampletype I-sep DL for differential extraction and purification with prepfiler express in the automate express DNA extraction system. Forensic Sci Int Genet Suppl Ser. 2017 Dec 1;6:e353–4.

43. Klein SB, Buoncristiani MR. Evaluating the efficacy of DNA differential extraction methods for sexual assault evidence. Forensic Sci Int Genet. 2017 Jul 1;29:109–17.

44. Mudariki T, Pallikarana-Tirumala H, Ives L, Hadi S, Goodwin W. A comparative study of two extraction methods routinely used for DNA recovery from simulated post coital samples. Forensic Sci Int Genet Suppl Ser. 2013 Jan 1;4(1):e194–5.

45. Goldstein MC, Cox JO, Seman LB, Cruz TD. Improved resolution of mixed STR profiles using a fully automated differential cell lysis/DNA extraction method. Forensic Sci Res [Internet]. 2020 Apr 2 [cited 2021 Dec 9];5(2):106–12. Available from: https://www.tandfonline.com/doi/abs/10.1080/20961790.2019.1646479

46. Knox C, Olson R. Tackling the Backlog Using Automated Differential Extraction | Office of Justice Programs. Forensic Mag [Internet]. 2008 [cited 2021 Dec 9];5(2). Available from: https://www.ojp.gov/ncjrs/virtual-library/abstracts/tackling-backlog-using-automated-differential-extraction

47. Anslinger K, Bayer B, Mack B, Eisenmenger W. Sex-specific fluorescent labelling of cells for laser microdissection and DNA profiling. Int J Legal Med [Internet]. 2007 Jan 18 [cited 2021 Dec 9];121(1):54–6. Available from: https://link.springer.com/article/10.1007/s00414-005-0065-7

48. Anslinger K, Mack B, Bayer B, Rolf B, Eisenmenger W. Digoxigenin labelling and laser capture microdissection of male cells. Int J Legal Med [Internet]. 2005 Nov 5 [cited 2021 Dec 9];119(6):374–7. Available from: https://link.springer.com/article/10.1007/s00414-005-0523-2

49. Axler-DiPerte G, Orans S, Singh A, Caragine T, Prinz M, Budimlja ZM. Comparison and optimization of DNA recovery from sperm vs. epithelial cells using laser capture microdissection technology and an immunofluorescent staining system. Forensic Sci Int Genet Suppl Ser. 2011 Dec 1;3(1):e224–5.

50. Fontana F, Rapone C, Bregola G, Aversa R, de Meo A, Signorini G, et al. Isolation and genetic analysis of pure cells from forensic biological mixtures: The precision of a digital approach. Forensic Sci Int Genet. 2017 Jul 1;29:225–41.

51. Horsman KM, Barker SLR, Ferrance JP, Forrest KA, Koen KA, Landers JP. Separation of Sperm and Epithelial Cells in a Microfabricated Device: Potential Application to Forensic Analysis of Sexual Assault Evidence. Anal Chem [Internet]. 2004 Feb 1 [cited 2021 Dec 9];77(3):742–9. Available from: https://pubs.acs.org/doi/abs/10.1021/ac0486239

52. Horsman KM, Bienvenue JM, Blasier KR, Landers JP. Forensic DNA Analysis on Microfluidic Devices: A Review. J Forensic Sci [Internet]. 2007 Jul 1 [cited 2021 Dec 9];52(4):784–99. Available from: https://onlinelibrary.wiley.com/doi/full/10.1111/j.1556-4029.2007.00468.x

53. Inci F, Ozen MO, Saylan Y, Miansari M, Cimen D, Dhara R, et al. A Novel On-Chip Method for Differential Extraction of Sperm in Forensic Cases. Adv Sci [Internet]. 2018 Sep 1 [cited 2021 Dec 9];5(9):1800121. Available from: https://onlinelibrary.wiley.com/doi/full/10.1002/advs.201800121

54. Chen J, Kobilinsky L, Wolosin D, Shaler R, Baum H. A Physical Method for Separating Spermatozoa from Epithelial Cells in Sexual Assault Evidence. J Forensic Sci [Internet]. 1998 Jan 1 [cited 2021 Nov 18];43(1):114–8. Available from: http://www.astm.org/DIGITAL_LIBRARY/JOURNALS/FORENSIC/PAGES/JFS16097J.htm

55. Anslinger K, Bayer B, Danilov SM, Metzger R. Application of sperm-specific antibodies for the separation

of sperm from cell mixtures. Forensic Sci Int Genet Suppl Ser. 2008 Aug 1;1(1):394–5.

56. Alsalafi D, Goodwin W. Capturing spermatozoa for STR analysis of sexual assault cases using anti-sperm antibodies. Forensic Sci Int Genet Suppl Ser. 2019 Dec 1;7(1):707–10.

57. Norris J V., Manning K, Linke SJ, Ferrance JP, Landers JP. Expedited, Chemically Enhanced Sperm Cell Recovery from Cotton Swabs for Rape Kit Analysis*. J Forensic Sci [Internet]. 2007 Jul 1 [cited 2021 Dec 9];52(4):800–5. Available from: https://onlinelibrary.wiley.com/doi/full/10.1111/j.1556-4029.2007.00453.x

58. Poland ML, Moghissi KS, Giblin PT, Ager JW, Olson JM. Variation of semen measures within normal men. Fertil Steril. 1985 Sep 1;44(3):396–400.

59. Eschenbach DA, Thwin SS, Patton DL, Hooton TM, Stapleton AE, Agnew K, et al. Influence of the Normal Menstrual Cycle on Vaginal Tissue, Discharge, and Microflora. Clin Infect Dis [Internet]. 2000 Jun 1 [cited 2021 Nov 18];30(6):901–7. Available from: https://academic.oup.com/cid/article/30/6/901/432360

60. Gaskins AJ, Mendiola J, Afeiche M, Jørgensen N, Swan SH, Chavarro JE. Physical activity and television watching in relation to semen quality in young men. Br J Sports Med [Internet]. 2015 Feb 1 [cited 2021 Nov 18];49(4):265–70. Available from: https://bjsm.bmj.com/content/49/4/265

61. Salas-Huetos A, Rosique-Esteban N, Becerra-Tomás N, Vizmanos B, Bulló M, Salas-Salvadó J. The Effect of Nutrients and Dietary Supplements on Sperm Quality Parameters: A Systematic Review and Meta-Analysis of Randomized Clinical Trials. Adv Nutr [Internet]. 2018 Nov 1 [cited 2021 Nov 18];9(6):833–48. Available from: https://academic.oup.com/advances/article/9/6/833/5194327

62. Comar VA, Petersen CG, Mauri AL, Mattila M, Vagnini LD, Renzi A, et al. Influence of the abstinence period on human sperm quality: analysisof 2,458 semen samples. JBRA Assist Reprod [Internet]. 2017 [cited 2021 Nov 18];21(4):306. Available from: /pmc/articles/PMC5714597/

63. Benschop CCG, Wiebosch DC, Kloosterman AD, Sijen T. Post-coital vaginal sampling with nylon flocked swabs improves DNA typing. Forensic Sci Int Genet. 2010 Feb 1;4(2):115–21.

64. Hudlow WR, Buoncristiani MR. Development of a rapid, 96-well alkaline based differential DNA extraction method for sexual assault evidence. Forensic Sci Int Genet. 2012 Jan 1;6(1):1–16.

65. Ma J, Tong Q, Gao L, Zhu C, Jiang Z. Extraction of DNA from Sperm Cells in Mixed Stain by Nylon Membrane Bushing Separation Technique. Fa Yi Xue Za Zhi [Internet]. 2018 Aug 25 [cited 2021 Jul 17];34(4):417–9. Available from: https://europepmc.org/article/med/30465410

66. Valgren C, Edenberger E. Evaluation of the Differex™ System. Forensic Sci Int Genet Suppl Ser. 2008 Aug 1;1(1):78–9.

67. Vuichard S, Borer U, Bottinelli M, Cossu C, Malik N, Meier V, et al. Differential DNA extraction of challenging simulated sexual-assault samples: a Swiss collaborative study. Investig Genet 2011 21 [Internet]. 2011 May 4 [cited 2021 Jul 19];2(1):1–7. Available from: https://link.springer.com/articles/10.1186/2041-2223-2-11

68. Barbisin M, Fang R, O'Shea CE, Calandro LM, Furtado MR, Shewale JG. Developmental validation of the Quantifiler Duo DNA Quantification kit for simultaneous quantification of total human and human male DNA and detection of PCR inhibitors in biological samples. J Forensic Sci [Internet]. 2009 Mar [cited 2022 Mar 11];54(2):305–19. Available from: https://pubmed.ncbi.nlm.nih.gov/19175708/

69. Holt A, Wootton SC, Mulero JJ, Brzoska PM, Langit E, Green RL. Developmental validation of the Quantifiler(®) HP and Trio Kits for human DNA quantification in forensic samples. Forensic Sci Int Genet [Internet]. 2016 Mar 1 [cited 2022 Mar 11];21:145–57. Available from: https://pubmed.ncbi.nlm.nih.gov/26774100/

70. Ewing MM, Thompson JM, McLaren RS, Purpero VM, Thomas KJ, Dobrowski PA, et al. Human DNA quantification and sample quality assessment: Developmental validation of the PowerQuant(®) system. Forensic Sci Int Genet [Internet]. 2016 Jul 1 [cited 2022 Mar 11];23:166–77. Available from: https://pubmed.ncbi.nlm.nih.gov/27206225/

71. Frégeau CJ, Laurin N. The Qiagen Investigator® Quantiplex HYres as an alternative kit for DNA quantification. Forensic Sci Int Genet [Internet]. 2015 [cited 2022 Mar 11];16:148–62. Available from: https://pubmed.ncbi.nlm.nih.gov/25603128/

72. Vandewoestyne M, Van Hoofstat D, Van Nieuwerburgh F, Deforce D. Suspension fluorescence in situ hybridization (S-FISH) combined with automatic detection and laser microdissection for STR profiling of male cells in male/female mixtures. Int J Legal Med [Internet]. 2009 Sep 25 [cited 2021 Nov 18];123(5):441–7. Available from: https://link.springer.com/article/10.1007/s00414-009-0341-z

73. Anslinger K, Bayer B, Mack B, Eisenmenger W. Sex-specific fluorescent labelling of cells for laser microdissection and DNA profiling. Int J Legal Med [Internet]. 2007 Jan 18 [cited 2021 Nov 18];121(1):54–6. Available from: https://link.springer.com/article/10.1007/s00414-005-0065-7

74. Di Martino D, Giuffrè G, Staiti N, Simone A, Le Donne M, Saravo L. Single sperm cell isolation by laser microdissection. Forensic Sci Int. 2004 Dec 2;146(SUPPL.):S151–3.

75. Elliott K, Hill DS, Lambert C, Burroughes TR, Gill P. Use of laser microdissection greatly improves the recovery of DNA from sperm on microscope slides. Forensic Sci Int. 2003 Oct 14;137(1):28–36.

76. Auka N, Valle M, Cox BD, Wilkerson PD, Cruz TD, Reiner JE, et al. Optical tweezers as an effective tool for spermatozoa isolation from mixed forensic samples. PLoS One [Internet]. 2019 Feb 1 [cited 2021 Nov 18];14(2):e0211810. Available from: https://journals.plos.org/plosone/article?id=10.1371/journal.pone.0211810

77. Hutchinson S, Chapman B, Turbett G. Sperm fishing: antigen-antibody complexes for the capture and enrichment of spermatozoa in mixed cell substrates. Aust J Forensic Sci [Internet]. 2019 Jul 29 [cited 2021 Jun 22];51(sup1):S95–8. Available from: https://www.tandfonline.com/action/journalInformation?journalCode=tajf20

78. Blackwell SJ, Mr S:, Chapman B. Forensic techniques for the isolation of sperm cells from mixed cell fractions: A review [Internet]. Murdoch University; 2017 [cited 2021 Jun 22]. Available from: https://researchrepository.murdoch.edu.au/id/eprint/39830/1/Blackwell2017.pdf

79. Roewer L, Epplen JT. Rapid and sensitive typing of forensic stains by PCR amplification of polymorphic simple repeat sequences in case work. Forensic Sci Int. 1992 Mar 1;53(2):163–71.

80. Katilius E, Carmel AB, Koss H, O'Connell D, Smith BC, Sanders GM, et al. Sperm cell purification from mock forensic swabs using SOMAmer^{TM} affinity reagents. Forensic Sci Int Genet. 2018 Jul 1;35:9–13.

81. Lauren S. How the immune system works [Internet]. 3rd ed. Oxford: Blackwell; 2008 [cited 2021 Nov 19]. Available from: https://library.lincoln.ac.uk/items/eds/cat04851a/uln.118022?resultsUri=items%3Fquery%3Dsubject%253A%2528immune%2Bsystem%2Bphysiopathology%2529%26offset%3D0%26target%3Deds

82. Wootla B, Denic A, Rodriguez M. Polyclonal and Monoclonal Antibodies in Clinic. Methods Mol Biol [Internet]. 2014 [cited 2021 Nov 19];1060:79–110. Available from: https://link.springer.com/protocol/10.1007/978-1-62703-586-6_5

83. Ámico DJD, Calne DB, Klawans HL. Altered hypothermic responsiveness to (+)-amphetamine. J Pharm Pharmacol. 1976;28(2):154–6.

84. Zhang H, Martin-DeLeon PA. Mouse Spam1 (PH-20) Is a Multifunctional Protein: Evidence for Its Expression in the Female Reproductive Tract. Biol Reprod [Internet]. 2003 Aug 1 [cited 2021 Nov 19];69(2):446–54. Available from: https://academic.oup.com/biolreprod/article/69/2/446/2712839

85. Ito C, Toshimori K. Acrosome markers of human sperm. Anat Sci Int. 2016;91:128–42.

86. Zhao XC, Wang L, Sun J, Jiang BW, Zhang EL, Ye J. Isolating Sperm from Cell Mixtures Using Magnetic Beads Coupled with an Anti-PH-20 Antibody for Forensic DNA Analysis. PLoS One [Internet]. 2016 Jul 1 [cited 2021 Nov 19];11(7):e0159401. Available from: https://journals.plos.org/plosone/article?id=10.1371/journal.pone.0159401

87. Jackson MB, Jackson M, Chapman B, Currie A. Developing Methods for Antibody-Mediated Enrichment and Capture of Spermatozoa from Complex Cell Mixtures for Forensics Applications. Murdoch University; 2019.

88. Yatsenko AN, O'Neil DS, Roy A, Arias-Mendoza PA, Chen R, Murthy LJ, et al. Association of mutations in the zona pellucida binding protein 1 (ZPBP1) gene with abnormal sperm head morphology in infertile men. Mol Hum Reprod [Internet]. 2012 Jan 1 [cited 2021 Nov 19];18(1):14–21. Available from: https://academic.oup.com/molehr/article/18/1/14/1080560

89. Maciorowski Z, Chattopadhyay PK, Jain P. Basic multicolor flow cytometry. Curr Protoc Immunol. 2017 Apr 1;2017:5.4.1-5.4.38.

90. Zhao XC, Wang L, Sun J, Jiang BW, Zhang EL, Ye J. Isolating Sperm from Cell Mixtures Using Magnetic Beads Coupled with an Anti-PH-20Antibody for Forensic DNA Analysis. PLoS One [Internet]. 2016 Jul 1 [cited 2021 Jun 22];11(7):e0159401. Available from: https://journals.plos.org/plosone/article?id=10.1371/journal.pone.0159401

91. Li XB, Wang QS, Feng Y, Ning SH, Miao YY, Wang YQ, et al. Magnetic bead-based separation of sperm

from buccal epithelial cells using a monoclonal antibody against MOSPD3. Int J Legal Med [Internet]. 2014 Nov 1 [cited 2021 Dec 10];128(6):905–11. Available from: https://link.springer.com/article/10.1007/s00414-014-0983-3

92. Sharpe JC, Evans KM. Advances in flow cytometry for sperm sexing. Theriogenology. 2009 Jan 1;71(1):4–10.

93. Cordelli E, Eleuteri P, Leter G, Rescia M, Spanò M. Flow cytometry applications in the evaluation of sperm quality: semen analysis, sperm function and DNA integrity. Contraception. 2005 Oct 1;72(4):273–9.

94. Spanò M, Bonde JP, Hjøllund HI, Kolstad HA, Cordelli E, Leter G. Sperm chromatin damage impairs human fertility. Fertil Steril. 2000 Jan 1;73(1):43–50.

95. Evenson DP, Jost LK, Marshall D, Zinaman MJ, Clegg E, Purvis K, et al. Utility of the sperm chromatin structure assay as a diagnostic and prognostic tool in the human fertility clinic. Hum Reprod [Internet]. 1999 Apr 1 [cited 2021 Dec 1];14(4):1039–49. Available from: https://academic.oup.com/humrep/article/14/4/1039/628788

96. World Health Organisation. WHO laboratory manual for the examination and processing of human semen [Internet]. 6th ed. 2021 [cited 2021 Nov 25]. Available from: https://www.who.int/publications/i/item/9789240030787

97. Cell Counting with a Hemocytometer | The Privalsky Lab @ UCDavis [Internet]. [cited 2021 Nov 25]. Available from: http://microbiology.ucdavis.edu/privalsky/hemocytometer

98. Before FlowJo™ | FlowJo, LLC [Internet]. [cited 2021 Dec 3]. Available from: https://www.flowjo.com/learn/flowjo-university/flowjo/before-flowjo/58

99. Linares R, Tan S, Gounou C, Arraud N, Brisson AR. High-speed centrifugation induces aggregation of extracellular vesicles. https://doi.org/103402/jev.v429509 [Internet]. 2015 [cited 2021 Dec 10];4(1). Available from: https://www.tandfonline.com/doi/abs/10.3402/jev.v4.29509

100. Stefanidou M, Alevisopoulos G, Spiliopoulou C. Fundamental Issues in Forensic Semen Detection. West Indian Med J. 2010;59(3).